RM-E9G08

Library

RESTRICTED

Copy 156
RM E9G08

NACA RM E9G08

TECHNICAL LIBRARY
AIRESEARCH MANUFACTURING CO.
9851-9951 SEPULVEDA BLVD.
INGLEWOOD,
CALIFORNIA

NACA

RESEARCH MEMORANDUM

ALTITUDE PERFORMANCE AND OPERATIONAL CHARACTERISTICS OF 29-INCH-DIAMETER TAIL-PIPE BURNER WITH SEVERAL FUEL SYSTEMS AND FLAME HOLDERS ON J35 TURBOJET ENGINE

By E. William Conrad and William R. Prince

Lewis Flight Propulsion Laboratory
Cleveland, Ohio

TECHNICAL LIBRARY
AIRESEARCH MANUFACTURING CO.
9851-9951 SEPULVEDA BLVD.
INGLEWOOD,
CALIFORNIA

CANCELLED
Classification CHANGED TO Unclassified
By authority Naca abstract - 1-27-54
Changed by Gus Date 2-4-54

CLASSIFIED DOCUMENT

This document contains classified information affecting the National Defense of the United States within the meaning of the Espionage Act, USC 50:31 and 32. Its transmission or the revelation of its contents in any manner to an unauthorized person is prohibited by law. Information so classified may be imparted only to persons in the military and naval services of the United States, appropriate civilian officers and employees of the Federal Government who have a legitimate interest therein, and to United States citizens of known loyalty and discretion who of necessity must be informed thereof.

NATIONAL ADVISORY COMMITTEE
FOR AERONAUTICS
WASHINGTON
November 8, 1949

RESTRICTED

NATIONAL ADVISORY COMMITTEE FOR AERONAUTICS

RESEARCH MEMORANDUM

ALTITUDE PERFORMANCE AND OPERATIONAL CHARACTERISTICS OF 29-INCH-DIAMETER TAIL-PIPE BURNER WITH SEVERAL FUEL SYSTEMS AND FLAME HOLDERS ON J35 TURBOJET ENGINE

By E. William Conrad and William R. Prince

SUMMARY

An investigation of turbojet-engine thrust augmentation by means of tail-pipe burning has been conducted in the NACA Lewis altitude wind tunnel. Several fuel systems and flame holders were investigated in a 29-inch-diameter tail-pipe burner to determine the effect of fuel distribution and flame-holder design on tail-pipe-burner performance and operational characteristics over a range of simulated flight conditions.

At an altitude of 5000 feet, the type of flame holder used had only a slight effect on the combustion efficiency. As the altitude was increased, the decrease in peak combustion efficiency became more rapid as the blocking area of the flame holder was reduced. At all altitudes investigated, an improvement in the uniformity of the radial distribution of fuel and air slightly increased the peak combustion efficiencies and shifted the peak combustion efficiency to higher tail-pipe fuel-air ratios. The use of an internal cooling liner extending the full length of the tail-pipe combustion chamber provided adequate shell cooling at all flight conditions investigated. At an altitude of 25,000 feet and rated engine speed, the ratio of augmented thrust to normal thrust increased from 1.44 at a flight Mach number of 0.27 to 1.67 at a flight Mach number of 0.92. The average specific fuel consumption increased from 2.48 to 2.55 pounds per hour per pound net thrust as the flight Mach number increased over this range of flight conditions. Operation was possible with most of the configurations up to an altitude of 45,000 feet at a flight Mach number of 0.27.

INTRODUCTION

In an extensive research program on thrust augmentation of turbojet engines being conducted at the NACA Lewis laboratory, utilization of the tail-pipe-burning cycle has been shown to be a practical method of increasing the thrust of turbojet engines (references 1 to 4). As part of this program, an investigation of thrust augmentation by means of tail-pipe burning was conducted with several axial-flow types of turbojet engine in the Lewis altitude wind tunnel. The work reported in references 1 to 4 was largely devoted to obtaining maximum thrust with high combustion efficiency and also stable burner operation over a wide range of fuel-air ratios and flight conditions. This investigation was conducted to study the effect of tail-pipe-burner design variables on burner performance and operation over a wide range of simulated flight conditions and thereby provide information that could be applied in designing tail-pipe burners. In order to obtain such information, it is necessary to determine the effect of flame holders, fuel systems, and burner dimensions on the burner requirements of maximum thrust with high combustion efficiency, stable burner operation over a wide range of fuel-air ratios and flight conditions, adequate tail-pipe cooling, dependable starting, and minimum loss in thrust with the burner inoperative.

In the phase of the tail-pipe-burning studies reported herein, several fuel systems and flame holders were investigated on a 29-inch-diameter tail-pipe burner used with an axial-flow turbojet engine to determine the effect of fuel distribution and flame-holder design on tail-pipe-burner performance and operating range. Tail-pipe-burner ignition systems and cooling liners were also investigated. Data were obtained with each configuration over a range of simulated flight conditions.

Comparative performance data are presented to show the effect on tail-pipe-burner combustion efficiency and exhaust-gas total temperature of (1) radial fuel distribution, (2) direction of fuel injection, and (3) type of flame holder. Data are presented in graphical and tabular form for the best configuration investigated to show the effect of altitude and flight Mach number on performance. Altitude blow-out characteristics, tail-pipe shell cooling, and tail-pipe fuel ignition are discussed.

APPARATUS AND INSTRUMENTATION

Engine

The J35 engine used in this investigation has a sea-level static thrust of 4000 pounds at an engine speed of 7700 rpm and a turbine-outlet temperature of 1250° F (1710° R). At this operating condition, the air flow is approximately 75 pounds per second. The over-all length of the standard engine and tail pipe is about 15 feet and the maximum diameter is about 38 inches. The main components of the standard engine include an 11-stage axial-flow compressor, eight cylindrical direct-flow combustors, a single-stage impulse turbine, a tail pipe, and an exhaust nozzle. The diameter of the standard exhaust nozzle used was $16\frac{15}{32}$ inches.

Throughout the investigation, AN-F-48b, grade 80, unleaded gasoline with a lower heating value of 19,000 Btu per pound and a hydrogen-carbon ratio of 0.186 was used in the tail-pipe burner and AN-F-32 fuel with a lower heating value of 18,550 Btu per pound and a hydrogen-carbon ratio of 0.155 was used in the engine.

Installation

The engine was mounted on a wing section that spanned the 20-foot-diameter test section of the altitude wind tunnel (fig. 1). Engine-inlet air pressures corresponding to altitude flight conditions were obtained by introducing dry refrigerated air from the tunnel make-up air system through a duct to the engine inlet. Air was throttled from approximately sea-level pressure to the desired pressure at the engine inlet, while the static pressure in the tunnel test section was maintained to correspond to the desired altitude. A slip joint with a frictionless seal was used in the duct, thereby making possible the measurement of thrust and installation drag with the tunnel scales. In order to simplify the installation, no cowling was installed.

Tail-Pipe-Burner Assembly

The standard 5-foot tail pipe was replaced by a tail-pipe-burner assembly 8 feet, 9 inches long, which was attached to the downstream flange of the turbine casing. A cross-sectional view of the tail-pipe-burner assembly with a typical flame holder and fuel system installed is shown in figure 2. The assembly consisted of three sections: (1) a diffuser section 30 inches long, tapering from an annular inlet area having an outside diameter of 34 inches to an outlet 29 inches in diameter and having an outlet- to inlet-area ratio of 1.75; (2) a cylindrical combustion chamber 29 inches in diameter and 48 inches long containing a cooling liner; and (3) a conical exhaust nozzle 27 inches long and $20\frac{3}{32}$ inches in diameter at the outlet. Because a variable-area nozzle satisfactory for tail-pipe burning was unavailable for this part of the program, a fixed conical exhaust nozzle was used. The diffuser section, the combustion-chamber shell, and the exhaust nozzle were constructed of 0.063-inch-thick Inconel. The downstream end of the diffuser inner body was cut off at a diameter of $8\frac{1}{2}$ inches and a cone having a depth of 4 inches was installed, thereby providing a turbulent region for seating a stabilizing flame in the center of the pipe. The cooling liner, which was constructed of 0.063-inch-thick Inconel, extended the full length of the combustion chamber. Between the liner and the burner shell was a radial space of 1/2 inch through which flowed a small quantity of the tail-pipe gas at approximately turbine-outlet temperature. The dimensions of the cooling liner were the same for all the configurations, but the method of support varied. 1158

Fuel systems and flame holders. - For all configurations the fuel was injected from 12 radial tubes equally spaced circumferentially and located in a plane $8\frac{1}{4}$ inches upstream of the diffuser outlet, which corresponds to a distance of $10\frac{3}{4}$ inches upstream of the flame holder and 7 inches upstream of the pilot cone. Four different sets of fuel injectors were used. Three sets were the impinging-jet type with 0.035-inch-diameter holes and were similar to those discussed in reference 3. The radial fuel distribution differed among the three sets, which are designated fuel patterns 1, 2, and 3 (fig. 3). The fourth set of fuel injectors had 0.035-inch-diameter holes drilled on both sides of the spray tubes to provide a fuel spray normal to the direction of gas flow. The holes were arranged in the same radial location as pattern 3. This injector arrangement is therefore designated side-spray-injector fuel pattern 3.

Three types of flame holder, which are designated as two-V, octagonal, and pilot flame holders (figs. 4 and 5), were used in the investigation. Three sizes of the two-V flame holder were used, which are designated small, medium, and large two-V flame holders, depending on the diameter of the outer ring (fig. 4). The octagonal flame holder had a semicircular cross section and was designed to approximate the semitoroidal flame holder used in the investigations discussed in references 3 and 4. The center pilot cone served as the flame holder for one of the configurations and also served as a part of the flame holder for the other configurations.

Eight configurations that included the aforementioned flame holders and fuel injectors were investigated. The flame holder and the fuel-injection system for each configuration are given in the following table:

Configuration	Flame holder	Flow area blocked by flame holder (percent)	Fuel-injection system
A	Small two-V	21.5	Impinging-jet injectors, fuel pattern 1; fuel injected in downstream direction
B	Small two-V	21.5	Impinging-jet injectors, fuel pattern 2; fuel injected in downstream direction
C	Medium two-V	23.0	Impinging-jet injectors, fuel pattern 3; fuel injected in downstream direction
D	Medium two-V	23.0	Impinging-jet injectors, fuel pattern 3; fuel injected in upstream direction
E	Medium two-V	23.0	Side-spray injectors, fuel pattern 3
F	Large two-V	29.2	Side-spray injectors, fuel pattern 3
G	Octagonal	18.9	Side-spray injectors, fuel pattern 3
H	Pilot	0	Side-spray injectors, fuel pattern 3

The flame-holder blocking area does not include the cross-sectional area of the pilot cone.

Ignition systems. - Two types of tail-pipe ignition system were investigated (fig. 6). For one system the fuel was injected through a conical spray fuel nozzle in the center of the pilot cone (system A). Two spark plugs were installed, one on either side of the pilot cone. The other system provided ignition by a momentary increase in fuel flow to the fuel nozzle in one of the engine combustors (system B). This excess fuel in one combustor caused a burst of flame through the turbine, thereby igniting the tail-pipe fuel. The tail-pipe-burner fuel pump was used as the source of high-pressure fuel for this system.

Instrumentation

Pressures and temperatures were measured at several stations in the engine and the tail-pipe burner. Engine air flow was measured with survey rakes mounted at the engine inlet. A complete pressure and temperature survey was obtained at the turbine outlet and total and static pressures at the tail-pipe-burner oulet were measured with a water-cooled survey rake. In order to obtain a correction to the scale thrust measurements, the drag of the water-cooled rake was determined by means of a hydraulic balance piston mechanism. Both engine and tail-pipe-burner fuel flows were measured by calibrated rotameters.

PROCEDURE

Data were obtained over a range of tail-pipe fuel flows at the following simulated flight conditions:

Altitude (ft)	Flight Mach number	Configuration							
5,000	0.26	A	B	C	D	E	F	G	H
10,000	.26							G	
15,000	.26				D		F		
15,000	.52		B						
25,000	.26	A	B	C	D	E	F	G	
25,000	.52		B		D		F		
25,000	.71		B		D	E	F		
25,000	.91		B	C	D		F	G	H
25,000	1.10		B						
30,000	.26							G	
35,000	.26	A	B		D		F	G	H
40,000	.26	A	B						
45,000	.26			C	D	E	F	G	H

Dry refrigerated air was supplied to the engine at standard NACA conditions, except that no temperatures below about -20° F were obtained. The total pressure at the engine inlet was regulated to the value corresponding to the desired flight condition assuming complete free-stream ram-pressure recovery.

At each flight condition with the engine operating at rated speed of 7700 rpm, the tail-pipe fuel flow was varied from a minimum determined by imminent blow-out to a maximum determined by (1) the limiting turbine-outlet temperature of 1250° F (1710° R), (2) a limitation of about 7200 pounds per hour of the fuel-supply system, or (3) rich combustion blow-out at high altitude.

Thrust measurements were obtained from the balance scales and from the pressure survey at the exhaust-nozzle outlet. The thrust values presented were obtained from the balance-scale measurements.

The jet-velocity coefficient may be defined as the ratio of actual (scale) jet thrust to the ideal thrust determined by measurements with the exhaust-nozzle survey rake. Variation of the jet-velocity coefficient with the nozzle pressure ratio is shown by the following curve for the conical exhaust nozzle used:

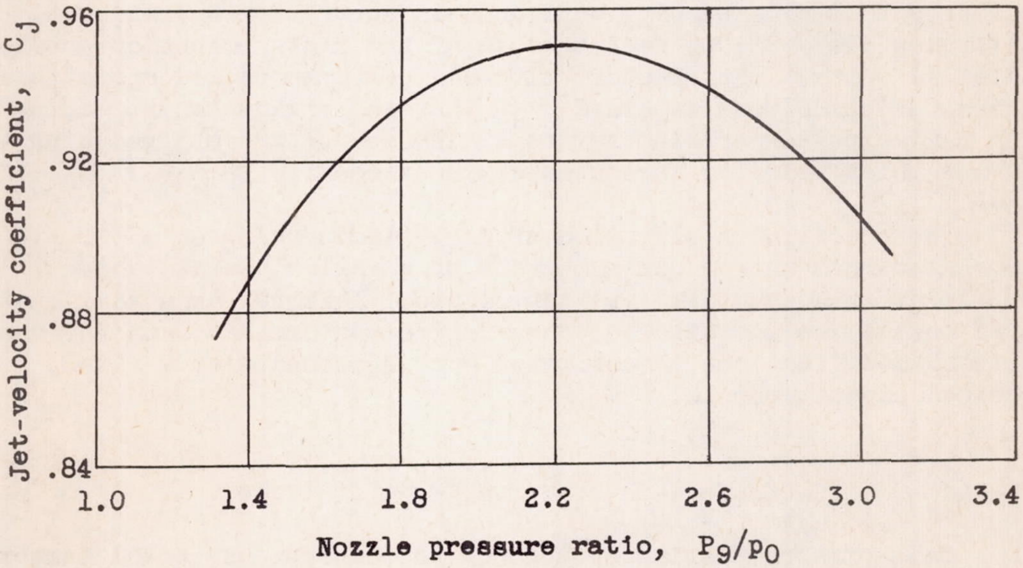

These values agree within the limit of data scatter with the values given in reference 5. The actual jet thrust for any other exhaust-nozzle design may be directly obtained by multiplying the thrust values presented by the ratio of the appropriate jet-velocity coefficient to the coefficient given by the curve.

Exhaust-gas temperature and combustion efficiency were based on the measurements at the exhaust-nozzle outlet. The probable limits of error in the absolute values of jet thrust, jet temperature, and tail-pipe combustion efficiency are $\pm 1\frac{1}{2}$, ±3, and ±5 percent, respectively. The symbols used in this report and the methods used in calculating the results are given in the appendix.

RESULTS AND DISCUSSION

Results of a preliminary phase of this investigation, in which several flame holders and fuel systems were used in a $25\frac{3}{4}$-inch-diameter tail-pipe burner, were unsatisfactory for operation at altitudes above 25,000 feet because of the high combustion-chamber-inlet velocity. Satisfactory altitude performance and operational characteristics were obtained with the same engine by increasing the tail-pipe-burner diameter to 29 inches and thereby reducing the burner-inlet velocity approximately 30 percent.

The practical application of tail-pipe burning as a thrust-augmentation means requires the use of a variable-area exhaust nozzle or a two-position exhaust nozzle. Inasmuch as a variable-area nozzle was unavailable, comparative performance data for the several modifications investigated were obtained with a fixed conical exhaust nozzle.

Comparison of Burner Modifications

Tail-pipe combustion efficiency and exhaust-gas total temperature were chosen as the variables to show the effect of radial fuel distribution, the direction of fuel injection, and the type of flame holder used. These variables are presented as a function of tail-pipe fuel-air ratio, which is defined as the ratio of tail-pipe fuel flow to the unburned air flow entering the tail pipe.

Radial fuel distribution. - The effect of varying the radial distribution of tail-pipe fuel is shown in figure 7, in which data for configurations A and B are compared. For configuration A with fuel pattern 1, each injector had four pairs of impinging jets; whereas, for configuration B with fuel pattern 2, each injector had three pairs of impinging jets. At all altitudes investigated, the more uniform radial mixture afforded by fuel pattern 1 gave slightly higher peak combustion efficiencies and increased the tail-pipe fuel-air ratio at which the peak combustion efficiency occurred. Both of these factors contributed to the higher exhaust-gas temperatures and the concomitant thrusts obtained with configuration A.

Direction of fuel injection. - The exposure time of the fuel to the hot gases in the tail pipe and the peripheral distribution of fuel might have an effect on combustion efficiency. The effect of the direction of fuel injection is shown in figure 8, in which data for configurations C, D, and E are compared. All three configurations had fuel pattern 3, which was a modification of fuel pattern 1 designed to give a more homogeneous radial mixture. The fuel was injected downstream from impinging-jet injectors for configuration C, upstream from impinging-jet injectors for configuration D, and sidewise from side-spray injectors for configuration E. At altitudes of 25,000 and 45,000 feet the direction of fuel injection had no appreciable effect on the combustion efficiency or the exhaust-gas total temperature.

Flame holders. - A comparison of the performance with four different flame holders is presented in figure 9, which shows data for configurations E, F, G, and H. Configuration E had the medium two-V flame holder, configuration F the large two-V flame holder, configuration G the octagonal flame holder, and configuration H the pilot flame holder. At an altitude of 5000 feet, the variations in combustion efficiency and exhaust-gas total temperature with the four flame holders were small. At this altitude the large and the medium two-V flame holders had approximately the same combustion efficiency and exhaust-gas total temperature at fuel-air ratios above 0.025. Above this fuel-air ratio, the combustion efficiency was about 0.05 lower with the octagonal flame holder than with the two-V flame holders and from 0.05 to 0.09 lower with the pilot flame holder than with the two-V flame holders. At an altitude of 45,000 feet, the variations in combustion efficiency and exhaust-gas total temperature with the four configurations were large. The maximum combustion efficiencies obtained at this altitude were 0.76 with the large two-V flame holder, 0.51 with the medium two-V flame holder, 0.37 with the octagonal flame holder, and 0.13 with the pilot flame holder. The corresponding exhaust-gas total temperatures varied in the same manner as the combustion efficiency.

The variation of the peak combustion efficiency with altitude for each configuration is shown in figure 10. These data indicate that at an altitude of 5000 feet the type of flame holder used had only a small effect on the combustion efficiency. In general, as the altitude was increased, the differences in combustion efficiency obtained with the four configurations became considerably greater. At all altitudes, the combustion efficiency decreased as the blocking area of the flame holder was reduced. The broken portions of the curve for configurations F and G were determined by peak efficiency values obtained by slightly extrapolating the curves of tail-pipe combustion efficiency as a function of tail-pipe fuel-air ratio.

Total-pressure-loss ratios across the standard tail pipe and the tail-pipe burners under nonburning conditions were measured, but the trends were inconclusive. The total-pressure-loss ratio is defined as the loss in total pressure between the burner inlet and the exhaust-nozzle outlet, divided by the burner-inlet total pressure. At rated engine speed, the total-pressure-loss ratio was 0.011 for the standard tail pipe and varied from 0.025 to 0.035 for the tail-pipe-burner configurations.

Performance Characteristics

From the data of figures 7 to 10 and from additional data not shown, the highest tail-pipe combustion efficiency and exhaust-gas total temperatures were obtained with configuration F. Data obtained with configuration F were therefore selected to demonstrate the effect of altitude and flight Mach number on these parameters. Data for configurations C, D, E, and F have been shown to illustrate the effect of flight Mach number on thrust-augmentation ratio, exhaust-gas total temperature, and specific fuel consumption. Data obtained with configuration F are presented in table I.

Tail-pipe-burner performance. - The effect of altitude on the variation of exhaust-gas total temperature, tail-pipe combustion efficiency, and burner- and combustion-chamber-inlet conditions with tail-pipe fuel-air ratio is shown in figure 11 for a range of altitudes at a flight Mach number of 0.27. The combustion efficiency at an altitude of 35,000 feet reached a peak value of 0.86 at tail-pipe fuel-air ratios between about 0.030 and 0.040, which correspond to over-all fuel-air ratios from 0.039 to 0.046. Increasing the altitude from 5000 to 35,000 feet resulted in slightly higher combustion efficiency (fig. 11(b)) and exhaust-gas total temperature (fig. 11(a)). These slight increases, however, may be due to discrepancies in the data. A further increase in altitude to 45,000 feet resulted in a slight reduction in combustion efficiency and exhaust-gas total temperature from those at 5000 feet. The marked reduction in these parameters as tail-pipe fuel-air ratio was reduced below about 0.025 was often associated with combustion blow-out on one or both rings of the flame holder.

With the fixed-area exhaust nozzle, the burner-inlet conditions varied with fuel-air ratio as shown in figures 11(c) to 11(e). In general, the tail-pipe-burner-inlet total temperature and pressure increased with tail-pipe fuel-air ratio, whereas the combustion-chamber-inlet velocity remained constant at about 412 feet per second. At a given tail-pipe fuel-air ratio, the burner-inlet total temperature varied only slightly with changes in altitude except for data at 5000 feet for fuel-air ratios below 0.030.

The effect of flight Mach number on the variation of exhaust-gas total temperature, tail-pipe combustion efficiency, and burner- and combustion-chamber-inlet conditions with tail-pipe fuel-air ratio is shown in figure 12 for a range of flight Mach numbers from 0.27 to 0.92 at an altitude of 25,000 feet. Variations in flight Mach number had little effect on the combustion efficiency except at fuel-air ratios below about 0.025 in the region of partial burner blow-out (fig. 12(b)). The maximum tail-pipe combustion efficiency of 0.86 occurred at all flight Mach numbers investigated at tail-pipe fuel-air ratios of about 0.030 to 0.040.

The exhaust-gas total temperature was only slightly affected by variations in flight Mach number in the range investigated. With configuration F the maximum exhaust-gas total temperature of 3200° R was obtained at a tail-pipe fuel-air ratio of about 0.048 (fig. 11(a)), which corresponds to an over-all fuel-air ratio of 0.053. The slope of the curves indicates that somewhat higher temperatures might be obtained at higher fuel-air ratios if the exhaust-nozzle area were increased.

Operation with a variable-area exhaust nozzle would normally result in constant burner-inlet conditions at all fuel-air ratios instead of the variations shown in figures 11(c) to 11(e) and 12(c) to 12(e). High burner-inlet temperature and pressure normally have a beneficial effect on combustion efficiency. At a given flight condition, optimum burner-inlet conditions exist at only one tail-pipe fuel-air ratio with a fixed-area exhaust nozzle; whereas operation with a variable-area exhaust nozzle would make possible optimum burner-inlet (turbine-outlet) conditions over a wide range of fuel-air ratios with corresponding improvements in performance.

Over-all performance. - Thrust, exhaust-gas total temperature, and specific fuel consumption were obtained for configurations C, D, E, and F (figs. 13 and 14) by cross-plotting the data for a turbine-outlet temperature of 1650° R, which was the highest temperature at which sufficient data were available for cross-plotting with little extrapolation. Calculations indicate that slightly higher thrust augmentation would be obtained in operation at the limiting turbine-outlet temperature of 1710° R. The performance data presented for these configurations are significant only for the size exhaust nozzle used. For the best configurations investigated, increasing the exhaust-nozzle area would permit operation at higher fuel-air ratios with attendant increases in thrust and exhaust-gas total temperature, although the specific fuel consumption would also be higher.

The variation of exhaust-gas total temperature and the ratio of augmented to normal net thrust with flight Mach number at an altitude of 25,000 feet is shown in figure 13. Augmented thrust is defined as the thrust with the tail-pipe burner installed and normal thrust is defined as the net thrust obtained at the same turbine-outlet conditions with the standard tail pipe. The ratio of augmented to normal thrust increased from 1.44 at a flight Mach number of 0.27 to 1.67 at a flight Mach number of 0.92. With this increase in flight Mach number, the exhaust-gas total temperature rose from 3165° to 3295° R. With the average total-pressure-loss ratio across the tail pipe of 0.030, the thrust with the tail-pipe burner inoperative was 0.98 of that obtained with the standard tail pipe.

Variation of the specific fuel consumption based on net thrust with flight Mach number with the tail-pipe burner operating and with the standard-engine tail pipe is shown in figure 14. With the burner operating, the average specific fuel consumption for the four configurations varied from 2.48 to 2.55 as the flight Mach number was increased from 0.27 to 0.92. The specific fuel consumption with the standard-engine tail pipe varied from 1.15 at a flight Mach number of 0.27 to 1.32 at a flight Mach number of 0.92.

Operating Range

The operable range of tail-pipe fuel-air ratios for configurations A to H is shown in figure 15 for altitudes from 15,000 to 45,000 feet and a flight Mach number of 0.27. At a given altitude, operation was possible over a range of tail-pipe fuel-air ratios from lean combustion blow-out, or the region of uncertain operation, to the tail-pipe fuel-air ratio corresponding to limiting turbine-outlet temperature. The region of uncertain operation represents a range of fuel-air ratios in which blow-out is likely to occur. The exact point of blow-out depends largely on the rate of throttle retraction. With configuration G, rich combustion blow-out was occasionally encountered at high altitudes. At an altitude of 15,000 feet, the region of uncertain operation occupied a range of tail-pipe fuel-air ratios from approximately 0.008 to 0.023. As the altitude was increased, lean combustion blow-out occurred at higher fuel-air ratios; at an altitude of 45,000 feet, lean blow-out was encountered at tail-pipe fuel-air ratios as high as 0.032.

Periscope observations downstream of the exhaust nozzle indicated that blow-out often occurred in steps with the first blow-out at the outer ring of the flame holder and the last blow-out at the center pilot. The data presented are for complete blow-out. With the variable-area nozzle, the combustion blow-out region might be shifted to lower fuel-air ratios because higher burner-inlet temperature and pressure would be obtained at all fuel-air ratios.

Tail-Pipe Fuel Ignition

Several methods of igniting the tail-pipe fuel were investigated; only three methods, however, proved to be reasonably successful. A method of igniting the tail-pipe fuel, which consistently provided ignition at all flight conditions, was a rapid acceleration of the engine that resulted in a burst of flame through the turbine and into the tail pipe. This method occasionally caused blow-out in the engine combustors at 45,000 feet. Although this method is satisfactory for experimental work, it is unsuitable for flight use.

A second method, system A (fig. 6) utilized the pilot cone at the downstream end of the diffuser inner body to provide a sheltered region in which to install a fuel nozzle and spark plugs. Fuel was supplied to the ignition region by the nozzle in the pilot cone and by the main fuel injectors. With this system, starts were possible at rated engine speed up to an altitude of 25,000 feet. Occasional starts were made between 35,000 and 45,000 feet. Because the spark plugs were subject to failure from vibration and high temperature, this system was unreliable.

A third method, system B (fig. 6), which proved to be the most satisfactory, was developed from the practice of accelerating the engine to provide a flame in the tail pipe. High-pressure fuel from the tail-pipe-burner fuel pump was momentarily injected into one of the engine combustors and a resultant burst of flame went through the turbine and into the tail pipe. Ignition of the fuel at altitudes up to 50,000 feet was certain on the first attempt provided that a combustible fuel-air mixture was present; all starts were accomplished in less than 2 seconds. When starts were attempted with tail-pipe fuel-air ratios too lean to ignite, the engine speed increased about 100 rpm as a result of the momentary increase in fuel flow into the engine. Although the system was satisfactory with the burner investigated, it might be inadequate on a burner installation having a considerably greater distance between the turbine and the fuel injectors. Satisfactory operation of this system required that the high-pressure fuel be approximately 200 pounds per square inch above the large-slot manifold pressure at low altitudes. This pressure differential could be reduced to about 100 pounds per square inch at 45,000 feet. Subsequent experiments have shown no deterioration of the turbine diaphragm after over 200 starts with this system.

Tail-Pipe Cooling

Some of the tail-pipe burners previously investigated (reference 3) that had no cooling liners installed became excessively hot and prolonged operation at high fuel-air ratios resulted in damage to the burner shell and the exhaust nozzle. Heat-transfer calculations have indicated the feasibility of cooling the burner shell by installing a cooling liner inside the burner shell and thereby providing a flow of gas at turbine-outlet temperature between the burner shell and the liner. The calculations indicated that a radial space between the liner and the shell of from 1/2 to 1 inch should be provided. Some doubt then existed, however, as to whether a liner extending the full length of the burner section would not fail because of excessive temperature. Several liners subsequently investigated extended from 17 to 48 inches ahead of the exhaust nozzle and provided a radial space between the liner and the shell of from 1/2 to 1 inch. A liner extending the full length of the burner section (48 in.) and with a 1/2-inch radial space between the liner and the burner shell provided adequate cooling. With this arrangement, about 6 percent of the gas leaving the turbine passed between the liner and the burner shell, maintaining a shell temperature below a maximum of about 1660° R for all flight conditions investigated. The liner temperatures were somewhat higher, but the liner could withstand such high temperatures because the stresses in it were very low.

The method of supporting the liner offered considerable trouble. The static pressure between the liner and the burner shell was slightly higher than the static pressure in the burner, which resulted in a force tending to collapse the liner. The liner could not be rigidly secured to the burner shell, however, because the differential expansion between the two surfaces resulted in severe warpage of the liner. The most adequate method of support found in this phase of the investigation consisted of seam-welding 1- by 1/2-inch angles, 0.065 inch thick, longitudinally along the outer surface of the liner, spaced about 4 inches apart around the circumference. The flame-holder supports passed through slots cut in the forward end of the liner, which permitted the liner to expand with respect to the burner shell, and longitudinal movement of the liner was prevented by tack welds at the rear of the liner. The longitudinal angles welded to the liner provided adequate stiffness to prevent collapsing of the liner by the static-pressure differential across it. Other improvements in methods of supporting the liner were found in a subsequent phase of the investigation.

SUMMARY OF RESULTS

The following results were obtained from an investigation of a 29-inch-diameter tail-pipe burner on a turbojet engine in the NACA Lewis altitude wind tunnel:

1. At an altitude of 5000 feet, the type of flame holder used had only a small effect on the combustion efficiency. The decrease in peak combustion efficiency as the altitude was increased became more rapid as the blocking area of the flame holder was reduced.

2. At all altitudes investigated, an improvement in the uniformity of the radial mixture of fuel and air slightly increased the peak combustion efficiencies and shifted the peak combustion efficiency to higher tail-pipe fuel-air ratios.

3. At altitudes of 25,000 and 45,000 feet, the direction in which the tail-pipe fuel was injected into the stream had no apparent effect on the combustion efficiency.

4. The maximum tail-pipe combustion efficiency obtained was 0.86. This efficiency was obtained over a range of flight Mach numbers from 0.27 to 0.92 at an altitude of 25,000 feet and at a flight Mach number of 0.27 at 35,000 feet with tail-pipe fuel-air ratios of 0.030 to 0.040, which correspond to over-all fuel-air ratios of 0.039 to 0.046.

5. The use of an internal cooling liner extending the full length of the combustion chamber (48 in.) and having a 1/2-inch gap between the liner and the burner shell provided adequate shell cooling at all flight conditions investigated.

6. At an altitude of 25,000 feet and a turbine-outlet temperature of 1650° R, the ratio of augmented thrust to normal thrust increased from 1.44 at a flight Mach number of 0.27 to 1.67 at a flight Mach number of 0.92. With this increase in flight Mach number, the burner-outlet temperature rose from 3165° to 3295° R and the average specific fuel consumption increased from 2.48 to 2.55 pounds per hour per pound net thrust.

7. Operation was possible with most of the tail-pipe-burner configurations investigated up to an altitude of 45,000 feet at a flight Mach number of 0.27.

8. Momentary injection of high-pressure fuel into one of the engine combustors provided satisfactory ignition of the tail-pipe fuel at altitudes up to 50,000 feet at maximum engine speed.

Lewis Flight Propulsion Laboratory,
National Advisory Committee for Aeronautics,
Cleveland, Ohio.

APPENDIX - METHODS OF CALCULATION

Symbols

The following symbols are used in the calculations and on the figures.

A	cross-sectional area, sq ft
B	thrust scale reading, lb
C_d	flow (discharge) coefficient, ratio of effective flow area to measured area
C_j	jet-velocity coefficient, ratio of actual jet velocity or thrust to ideal velocity or thrust after expansion to free-stream static pressure
C_n	nozzle coefficient, $C_d C_j$
C_T	thermal-expansion ratio, ratio of hot-exhaust-nozzle area to cold-exhaust-nozzle area
D	external drag of installation, lb
D_r	drag of exhaust-nozzle survey rake, lb
F_j	jet thrust, lb
F_n	net thrust, lb
f/a	fuel-air ratio
g	acceleration due to gravity, 32.2 ft/sec^2
H	enthalpy, Btu/lb
h_c	lower heating value of fuel, Btu/lb
M	Mach number
P	total pressure, lb/sq ft absolute
P_8'	total pressure at exhaust-nozzle survey station in standard-engine tail pipe, lb/sq ft absolute
p	static pressure, lb/sq ft absolute

R	gas constant, 53.4 ft-lb/(lb)(°R)
T	total temperature, °R
t	static temperature, °R
V	velocity, ft/sec
W_a	air flow, lb/sec
W_c	bearing cooling air flow, lb/sec
W_f	fuel flow, lb/hr
W_f/F_n	specific fuel consumption based on total fuel flow and net thrust, lb/(hr)(lb thrust)
W_g	gas flow, lb/sec
γ	ratio of specific heats for gases
η_b	combustion efficiency

Subscripts:

a	air
e	engine
f	fuel
i	indicated
m	temperature of fuel in manifold
s	scale
t	tail-pipe burner
x	inlet duct at frictionless slip joint
0	free-stream conditions
1	engine inlet
6	tail-pipe burner inlet or turbine outlet

7	tail-pipe combustion-chamber inlet
8	exhaust nozzle, 1 in. forward of outlet
9	exhaust-nozzle outlet

Calculations

Flight Mach number and airspeed. - Flight Mach number and equivalent airspeed were calculated from the ram pressure ratio by use of the following equation:

$$M_0 = \sqrt{\frac{2}{\gamma-1}\left[\left(\frac{P_1}{p_0}\right)^{\frac{\gamma-1}{\gamma}} - 1\right]} \tag{1}$$

$$V_0 = M_0\sqrt{\gamma g R\, T_{i,1}\left(\frac{p_0}{P_1}\right)^{\frac{\gamma-1}{\gamma}}} \tag{2}$$

The equivalent free-stream total temperature was assumed equal to engine-inlet indicated temperature. The use of this assumption introduces an error in airspeed of less than 1 percent.

Air flow. - Air flow through the engine was determined from the pressures and the temperatures measured at the engine inlet.

$$W_a = p_1 A_1 \sqrt{\frac{2\gamma g\left[\left(\frac{P_1}{p_1}\right)^{\frac{\gamma-1}{\gamma}} - 1\right]}{(\gamma-1)Rt_1}} \tag{3}$$

Static temperature was obtained from the indicated temperature by the use of an impact recovery factor of 0.85. A small quantity of air approximately equal to the engine fuel flow was bled from the compressor for bearing cooling and was taken into account in calculating the combustion efficiency and the tail-pipe fuel-air ratio.

Tail-pipe gas flow. - The total weight flow through the tail-pipe burner was calculated as

$$W_g = W_a + \frac{W_{f,e} + W_{f,t}}{3600} - W_c \tag{4}$$

Augmented thrust. - The thrust of the installation was independently determined from balance-scale measurements and from pressures measured near the exhaust-nozzle outlet by means of a water-cooled survey rake. Because of the inefficiency of the exhaust nozzle, the scale thrust is less than the rake thrust.

Jet thrust was determined from the balance-scale measurements by use of the following equation:

$$F_{j,s} = B + D + D_r + \frac{W_a V_x}{g} + A_x(p_x - p_0) \tag{5}$$

The last two terms represent momentum and pressure forces on the installation at the frictionless slip joint in the make-up air duct. The external drag of the installation was determined from experiments with the engine inoperative and with a blind flange installed to prevent air flow through the engine.

Rake thrust, which is the ideal thrust available, is given by the following equation based on the total pressures obtained at station 8, 1 inch upstream of the exhaust-nozzle outlet:

$$F_{j,8} = \frac{2C_T A_8 p_8 \gamma_9}{\gamma_9 - 1}\left[\left(\frac{P_8}{p_8}\right)^{\frac{\gamma_9 - 1}{\gamma_9}} - 1\right] + A_8 C_T (p_8 - p_0) \tag{6}$$

The value of γ_9 was obtained from an approximate exhaust-nozzle-outlet temperature calculated from scale thrust. Values of C_T were obtained from reference 6 and measured exhaust-nozzle skin temperatures. At the maximum exhaust-gas total temperature of 3300° R, the value of C_T was 1.024. Inasmuch as the static pressure p_8 was obtained for only part of the data, the following equations were also used to determine rake thrust. For supersonic jet velocity,

$$F_{j,9} = \frac{2C_T C_d A_9 p_9 \gamma_9}{\gamma_9 - 1}\left[\left(\frac{P_8}{p_9}\right)^{\frac{\gamma_9 - 1}{\gamma_9}} - 1\right] + C_d C_T A_9 (p_9 - p_0) \tag{7}$$

where

$$p_9 = \frac{P_9}{\left(\frac{\gamma_9 + 1}{2}\right)^{\frac{\gamma_9}{\gamma_9 - 1}}}$$

For subsonic jet velocity,

$$F_{j,9} = \frac{2C_T C_d A_9 p_0 \gamma_9}{\gamma_9 - 1}\left[\left(\frac{P_8}{p_0}\right)^{\frac{\gamma_9 - 1}{\gamma_9}} - 1\right] \tag{8}$$

where

$$p_9 = p_0$$

The change in total pressure between the measuring station and the exhaust-nozzle outlet was assumed to be negligible.

Net thrust was obtained from jet thrust by the use of the equation

$$F_n = F_j - \frac{W_a}{g} V_0 \tag{9}$$

The flow coefficient C_d used in equations (7) and (8) was obtained as follows: The jet thrust given by equation (6) was plotted as a function of P_8/p_0 for all the data containing a value of p_8. The appropriate expression for jet thrust given by equations (7) and (8) with C_d omitted, was plotted on the same figure.

The flow coefficient C_d was then obtained as the ratio of the ordinates of the two curves.

In a similar manner, the combined nozzle coefficient C_n was obtained as the ratio of the scale jet thrust (equation (5)) to the jet thrust given by equations (7) and (8) with C_d omitted. The jet-velocity coefficient is given by

$$C_j = \frac{C_n}{C_d} \tag{10}$$

The values of thrust presented were obtained by use of equation (5), which includes nozzle losses.

Exhaust-gas temperature. - Values of exhaust-gas total-temperature at the tail-pipe-burner outlet were determined by use of the equation

$$T_9 = \left(\frac{A_9 C_d C_T p_9}{W_g}\right)^2 \frac{2g}{R}\left(\frac{\gamma_9}{\gamma_9 - 1}\right)\left[\left(\frac{p_8}{p_9}\right)^{\frac{\gamma_9 - 1}{\gamma_9}} - 1\right]\left(\frac{p_8}{p_9}\right)^{\frac{\gamma_9 - 1}{\gamma_9}} \tag{11}$$

Turbine-outlet temperature. - Because the temperature measurements at station 6 were unreliable when the tail-pipe burner was in operation, the turbine-outlet temperatures given in table I were calculated by means of the following relation:

$$H_6 = \frac{H_{a,1}\ (W_a - W_c) + \left(\frac{W_{f,e}}{3600}\right) h_c\ \eta_{b,e}}{W_a + \frac{W_{f,e}}{3600} - W_c} \tag{12}$$

The value of T_6 was then obtained from H_6 and enthalpy charts. The engine combustion efficiency $\eta_{b,e}$ was determined from experiments without tail-pipe burning to be approximately 98 percent at rated engine speed.

Combustion-chamber-inlet velocity. - The velocity at the combustion-chamber inlet was calculated from the continuity equation using the static pressure measured immediately upstream of the flame holder and assuming constant total pressure and temperature from the turbine outlet to the burner inlet as follows:

$$V_7 = \frac{W_g R T_6}{p_7 A_7} \left(\frac{p_7}{P_6}\right)^{\frac{\gamma_6 - 1}{\gamma_6}} \tag{13}$$

Combustion efficiency. - Tail-pipe combustion efficiency was calculated by the equation

$$\eta_{b,t} = \frac{3600\left(W_a - W_c\right) H_a\Big]_1^9 + W_{f,e}\, H_{f,e}\Big]_m^9 + W_{f,t}\, H_{f,t}\Big]_m^9 - W_{f,e}\, h_{c,e}}{W_{f,t}\, h_{c,t}} \tag{14}$$

The engine fuel is assumed to be burned completely in the engine. Dissociation has not been considered in the calculation of combustion efficiency; however, up to temperatures of 3600° R the effect of dissociation is negligible. The method of determining the enthalpy of fuel is given in reference 7.

Tail-pipe fuel-air ratio. - The tail-pipe fuel-air ratio is defined as the ratio of the tail-pipe fuel flow to the unburned air entering the tail-pipe burner. The assumption used in obtaining this equation was that the fuel injected in the engine was completely burned.

$$\left(\frac{f}{a}\right)_t = \frac{W_{f,t}}{3600\left(W_a - W_c\right) - \frac{W_{f,e}}{0.067}} \tag{15}$$

The value of 0.067 is the stoichiometric fuel-air ratio for the fuel used.

Normal thrust. - In order to account for the possible performance deterioration in the basic engine during the progress of the tail-pipe-burning program, the normal net thrust at rated engine speed was calculated from measurements of total pressure and temperature at the turbine outlet, the gas flow leaving the turbine, and the total-pressure-loss ratio across the standard tail pipe. The method of calculating this thrust is shown in the following equation:

$$F_n = \frac{C_j\left(W_a - W_c + \frac{W_{f,e}}{3600}\right)}{g}\sqrt{\frac{2\gamma_6}{\gamma_6 - 1}\, gRT_6\left[1 - \left(\frac{p_0}{P_8'}\right)^{\frac{\gamma_6 - 1}{\gamma_6}}\right]} - \frac{W_a}{g} V_0 \qquad (16)$$

where P_8' is the product of P_6 and the total-pressure ratio across the standard tail pipe P_8/P_6 at rated engine speed. A value of 0.97 was used for C_j in determining the actual thrust of the basic engine.

REFERENCES

1. Fleming, W. A., and Dietz, R. O.: Altitude-Wind-Tunnel Investigations of Thrust Augmentation of a Turbojet Engine. I - Performance with Tail-Pipe Burning. NACA RM E6I20, 1946.

2. Fleming, William A., and Golladay, Richard L.: Altitude-Wind-Tunnel Investigation of Thrust Augmentation of a Turbojet Engine. III - Performance with Tail-Pipe Burning in Standard-Size Tail Pipe. NACA RM E7F10, 1947.

3. Fleming, William A., and Wallner, Lewis E.: Altitude-Wind-Tunnel Investigation of Tail-Pipe Burning with a Westinghouse X24C-4B Axial-Flow Turbojet Engine. NACA RM E8J25e, 1948.

4. Lundin, Bruce T., Dowman, Harry W., and Gabriel, David S.: Experimental Investigation of Thrust Augmentation of a Turbojet Engine at Zero Ram by Means of Tail-Pipe Burning. NACA RM E6J21, 1947.

5. Grey, R. E., and Wilsted, H. D.: Performance of Conical Jet Nozzles in Terms of Flow and Velocity Coefficients. NACA TN 1757, 1948.

6. Anon.: Engineering Properties of Inconel. Bull. T-7, Development and Res. Div., The International Nickel Co., Inc., March 1943.

7. Turner, L. Richard, and Lord, Albert M.: Thermodynamic Charts for the Computation of Combustion and Mixture Temperatures at Constant Pressure. NACA TN 1086, 1946.

TABLE I - PERFORMANCE DATA WITH TAIL-PIPE BURNER CONFIGURATION F

Run	Altitude (ft)	Flight Mach number M_0	Free-stream static pressure, p_0 (lb/sq ft abs.)	Engine-inlet total pressure, P_1 (lb/sq ft abs.)	Engine-inlet total temperature, T_1, ($^{\circ}$R)	Engine fuel flow $W_{f,e}$, (lb/hr)	Tail-pipe fuel flow $W_{f,t}$, (lb/hr)	Jet thrust, F_j (lb)	Net thrust, F_n (lb)	Air flow, W_a (lb/sec)	Specific fuel consumption, W_f/F_n (lb/(hr)(lb thrust))	Total fuel-air ratio, f/a	Tail-pipe fuel-air ratio, $(f/a)_t$	Tail-pipe combustion efficiency, $\eta_{b,t}$	Turbine-outlet total pressure, P_6 (lb/sq ft abs.)	Turbine-outlet total temperature, T_6, ($^{\circ}$R)	Combustion-chamber inlet static pressure, p_7 (lb/sq ft abs.)	Exhaust-nozzle total pressure, P_8 (lb/sq ft abs.)	Exhaust-gas total temperature, T_9, ($^{\circ}$R)	Run
1	5,000	0.270	1741	1831	517	3260	5200	4155	3571	62.86	2.25	0.0379	0.0299	0.762	3190	1530	3057	3034	2609	1
2	5,000	.276	1766	1861	521	2900	4100	3528	2925	63.45	2.23	.0311	.0226	.679	3003	1415	2867	2857	2210	2
3	5,000	.287	1762	1866	509	2140	2580	2226	1590	65.02	2.55	.0203	.0129	.213	2543	1170	2401	2459	1345	3
4	5,000	.270	1748	1839	506	3590	6118	4679	4087	64.41	2.27	.0425	.0352	.790	3394	1585	3260	3232	2835	4
5	15,000	.277	1191	1257	469	2690	4600	3628	3201	47.01	2.15	.0438	.0366	.814	2512	1585	2402	2378	2911	5
6	15,000	.273	1184	1247	475	2345	3510	3151	2736	46.12	2.04	.0357	.0274	.821	2304	1472	2195	2183	2556	6
7	15,000	.273	1184	1247	478	2020	3010	2542	2128	45.90	2.43	.0308	.0227	.437	1968	1350	1856	1872	1876	7
8	15,000	.267	1188	1248	477	2500	4040	3371	2965	46.00	2.09	.0401	.0323	.839	2405	1538	2295	2276	2789	8
9	15,000	.265	1191	1251	480	2720	4970	3624	3220	45.92	2.26	.0473	.0409	.793	2514	1630	2404	2377	3030	9
10	15,000	.270	1188	1250	481	1500	2090	1562	1152	45.79	2.46	.0220	.0149	.267	1774	1142	1667	1716	1386	10
11	25,000	.270	782	823	446	1740	2780	2408	2132	32.00	2.01	.0398	.0319	.837	1658	1512	1580	1567	2753	11
12	25,000	.267	782	822	449	1500	2220	1992	1720	31.78	1.96	.0330	.0246	.782	1531	1384	1449	1445	2361	12
13	25,000	.276	782	824	452	1045	1755	1203	922	31.70	2.60	.0247	.0180	.252	1222	1116	1142	1170	1391	13
14	25,000	.273	775	816	452	1640	2470	2225	1950	31.38	1.96	.0369	.0286	.860	1598	1475	1516	1509	2650	14
15	25,000	.265	782	821	452	960	1220	972	702	31.58	2.46	.0193	.0124	.142	1155	1073	1074	1107	1183	15
16	25,000	.523	782	942	454	1660	2530	2477	1880	36.13	2.04	.0326	.0245	.769	1711	1350	1618	1614	2324	16
17	25,000	.528	779	942	456	2065	3700	3142	2540	36.03	2.14	.0452	.0384	.864	1951	1573	1861	1841	3038	17
18	25,000	.505	779	927	455	2000	3440	2995	2427	35.50	2.12	.0432	.0360	.853	1888	1555	1800	1783	2932	18
19	25,000	.533	779	945	455	1890	3020	2870	2260	36.19	2.05	.0382	.0303	.849	1840	1480	1751	1738	2694	19
20	25,000	.524	782	943	457	1100	1990	1480	882	36.01	2.90	.0241	.0178	.262	1321	1080	1242	1268	1365	20
21	25,000	.525	782	944	456	1020	1510	1270	670	36.09	2.88	.0196	.0133	.189	1262	1035	1173	1209	1196	21
22	25,000	.725	782	1109	470	2400	4490	3920	2978	41.41	2.19	.0470	.0407	.845	2248	1600	2152	2126	3099	22
23	25,000	.726	782	1110	472	2155	3580	3530	2586	41.33	2.07	.0391	.0314	.855	2108	1490	2010	1992	2759	23
24	25,000	.727	782	1111	474	1540	2750	2502	1559	41.16	2.39	.0293	.0223	.524	1729	1223	1632	1645	1877	24
25	25,000	.727	786	1117	474	2280	4010	3715	2766	41.40	2.11	.0428	.0357	.873	2191	1544	2094	2072	2961	25
26	25,000	.719	782	1103	477	1250	2310	1959	1034	40.68	2.89	.0245	.0183	.314	1504	1098	1405	1438	1447	26
27	25,000	.716	782	1100	473	1060	1800	1535	613	40.82	3.43	.0196	.0139	.146	1364	1009	1265	1304	1140	27
28	25,000	.921	782	1353	494	1620	3000	2939	1545	48.41	2.47	.0268	.0203	.469	1954	1170	1838	1834	1716	28
29	25,000	.926	796	1384	493	2570	4310	----	----	49.60	----	.0391	.0314	----	----	1510	----	----	----	29
30	25,000	.921	789	1365	493	2190	3510	3939	2532	48.92	2.02	.0328	.0249	.801	2295	1380	2182	2171	2399	30
31	25,000	.921	782	1353	495	1200	2500	2213	819	48.33	3.71	.0214	.0162	.157	1612	995	1490	1524	1167	31
32	25,000	.919	782	1349	496	1060	2000	1810	425	48.10	4.37	.0178	.0128	.059	1499	905	1372	1414	1006	32
33	35,000	.260	497	521	441	1200	2080	1627	1461	20.17	2.10	.0459	.0391	.848	1105	1601	1050	1039	3039	33
34	35,000	.267	493	518	441	1105	1700	1458	1288	20.05	2.01	.0394	.0313	.852	1044	1524	988	981	2752	34
35	35,000	.273	490	516	442	1000	1500	1339	1166	19.94	1.99	.0353	.0270	.793	991	1428	933	928	2480	35
36	35,000	.273	493	519	441	1280	2510	1743	1569	20.09	2.31	.0533	.0486	.771	1138	1679	1078	1068	3205	36
37	45,000	.246	305	318	452	660	1080	823	729	11.92	2.16	.0412	.0335	.762	628	1533	586	582	2704	37
38	45,000	.255	305	319	458	710	1240	886	788	11.83	2.32	.0466	.0398	.721	635	1622	602	596	2866	38
39	45,000	.263	305	320	469	600	940	720	620	11.65	2.17	.0372	.0291	.850	596	1480	554	550	2666	39

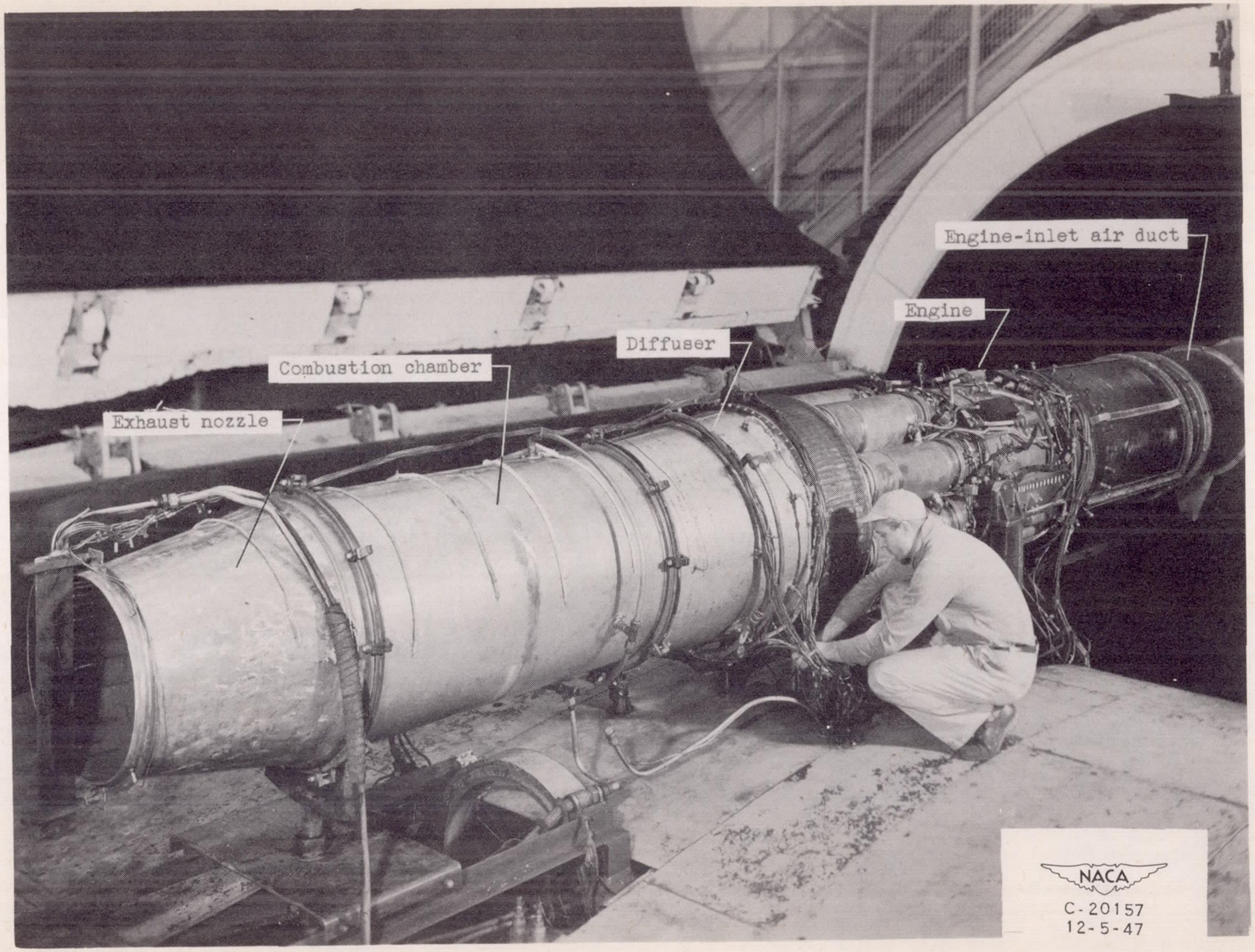
Engine-inlet air duct
Engine
Diffuser
Combustion chamber
Exhaust nozzle
NACA
C-20157
12-5-47

Figure 1. - Installation of engine and tail-pipe burner in altitude wind tunnel.

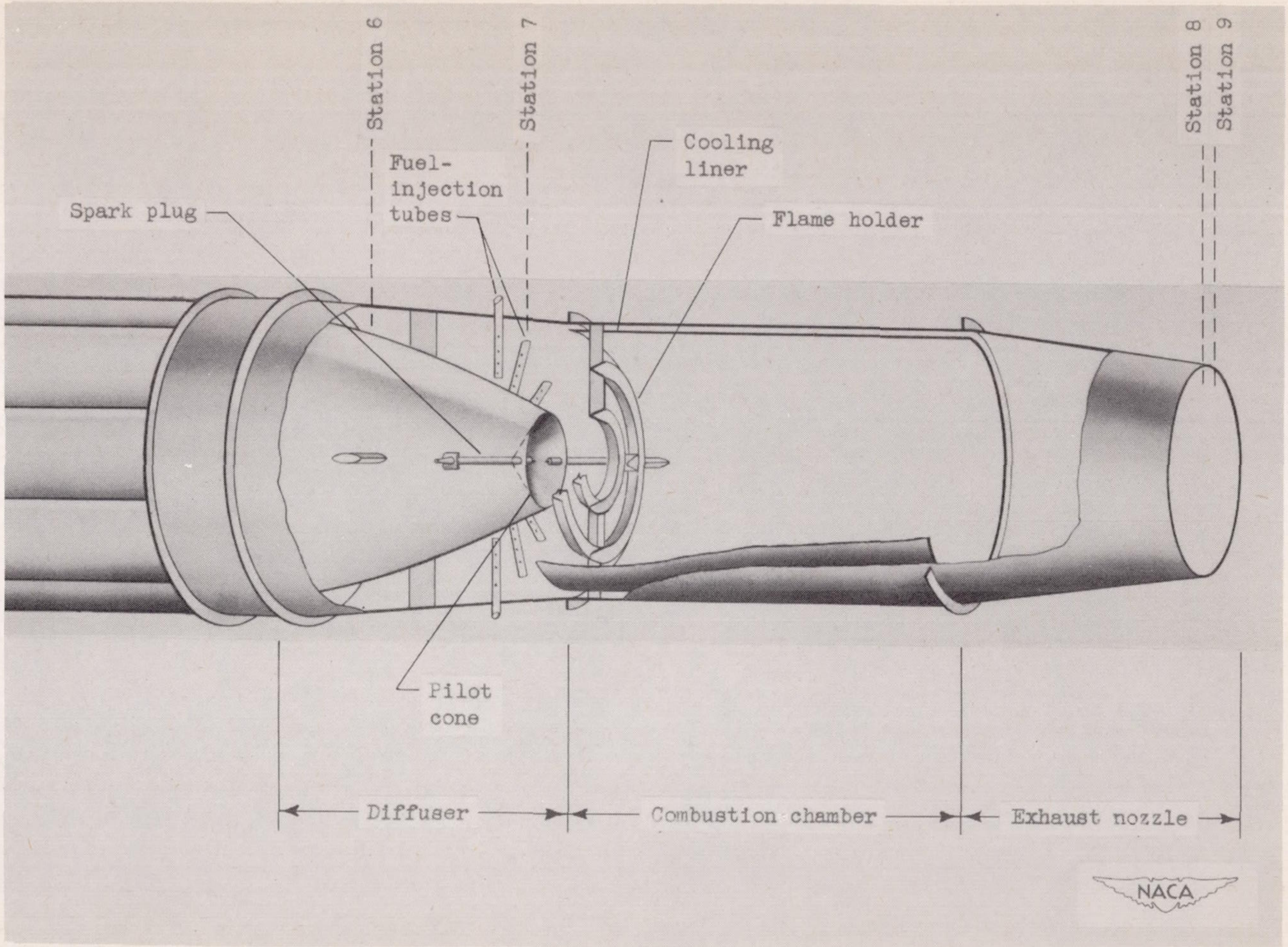
Station 6
Station 7
Station 8
Station 9
Fuel-injection tubes
Cooling liner
Spark plug
Flame holder
Pilot cone
Diffuser
Combustion chamber
Exhaust nozzle
NACA

Figure 2. - Cross-sectional view of typical tail-pipe-burner assembly.

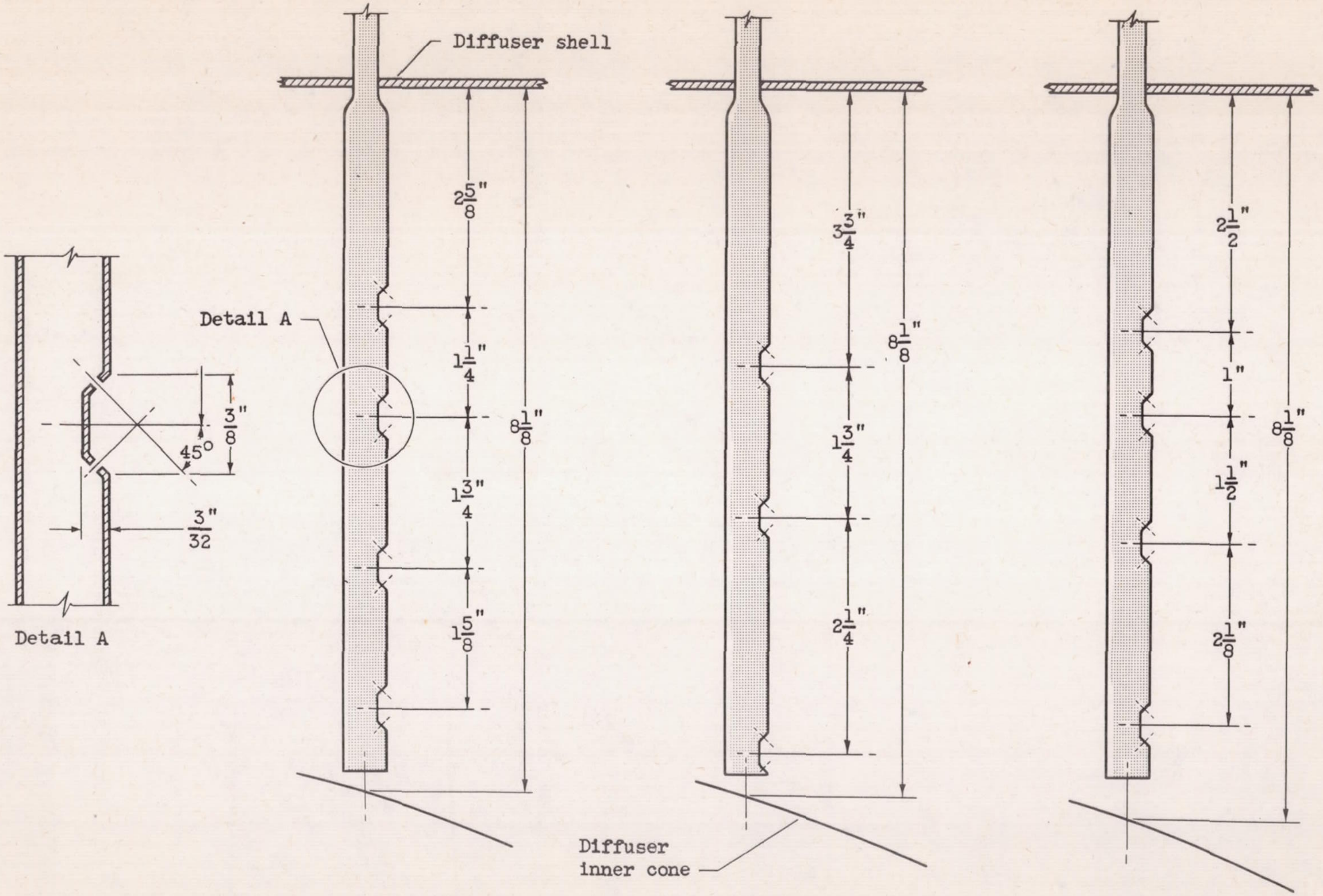
Diffuser shell
Detail A
3/8"
45°
3/32"
Detail A
2 5/8"
1 1/4"
1 3/4"
1 5/8"
8 1/8"
3 3/4"
8 1/8"
1 3/4"
2 1/4"
2 1/2"
1"
1 1/2"
2 1/8"
8 1/8"
Diffuser inner cone

Fuel pattern 1

Fuel pattern 2

Fuel pattern 3

Figure 3. - Impinging-jet fuel injectors.

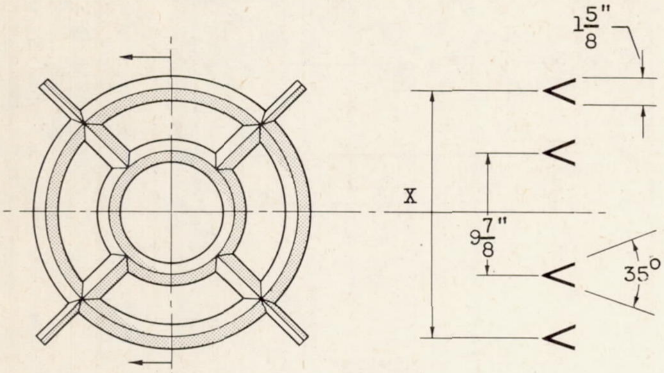
$1\frac{5}{8}$"
X
$9\frac{7}{8}$"
35°

Flame holder	Dimension X,(in.)
Small two-V	$16\frac{1}{8}$
Medium two-V	$18\frac{9}{16}$
Large two-V	$21\frac{1}{4}$

(a) Two-V flame holder.

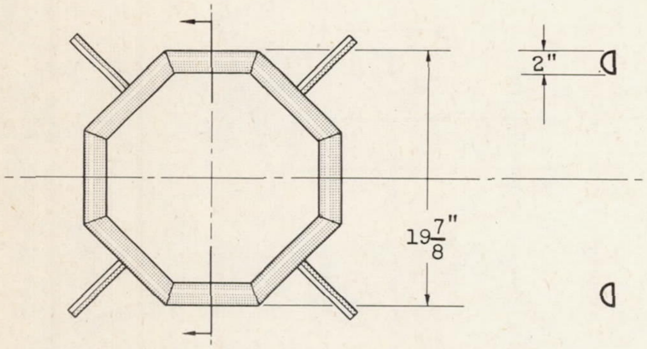

(b) Octagonal flame holder.

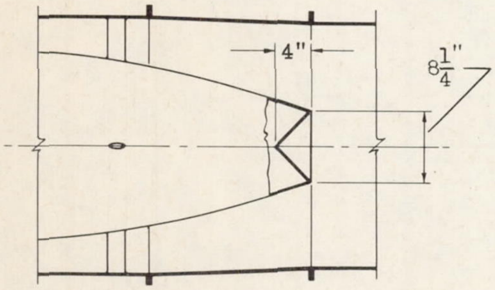

(c) Pilot flame holder.

Figure 4. - Schematic diagrams of flame holders.

206-1603

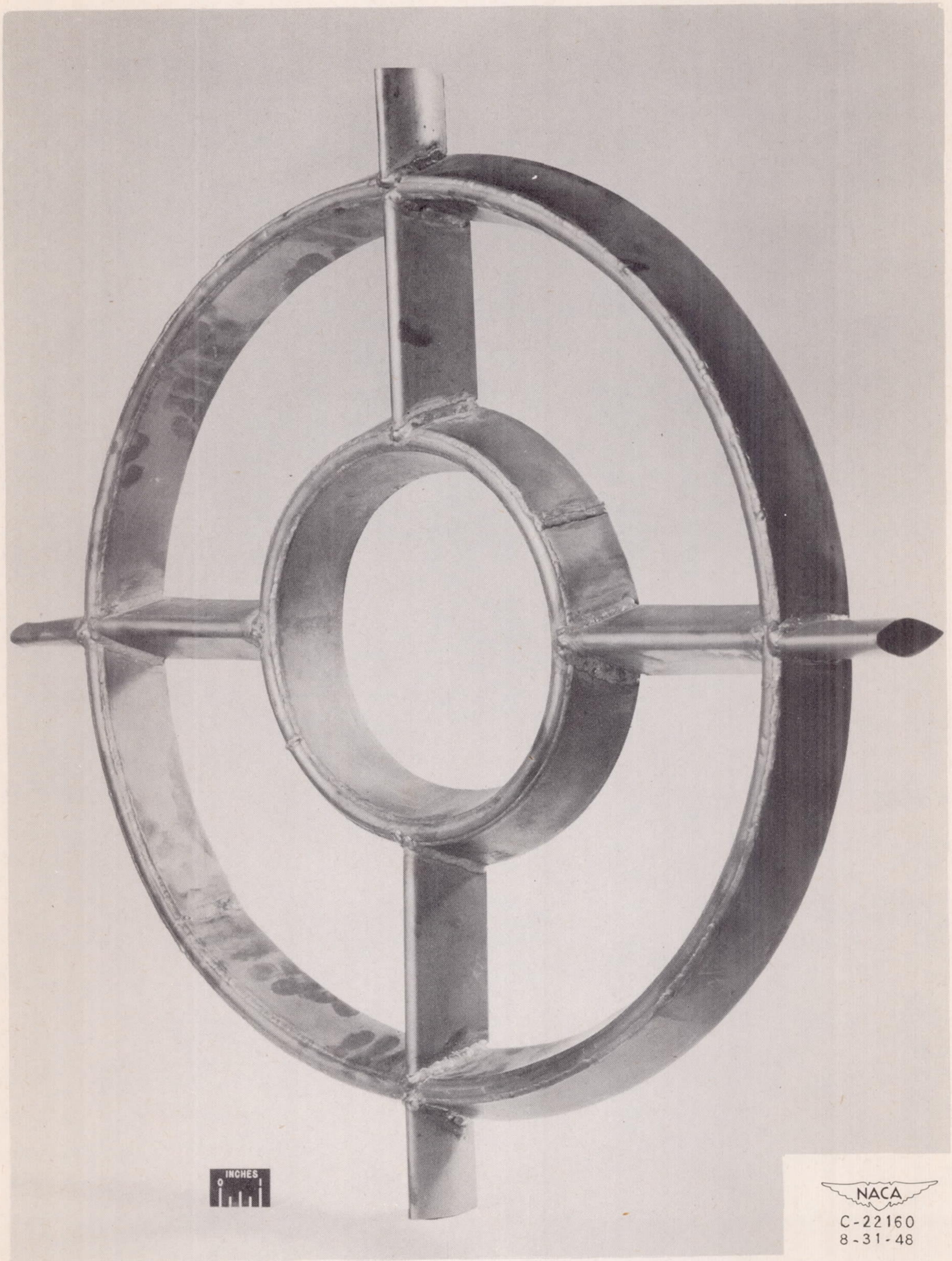
INCHES
0
1
NACA
C-22160
8-31-48

(a) Large two-V flame holder.
Figure 5. - Photographs of flame holders.

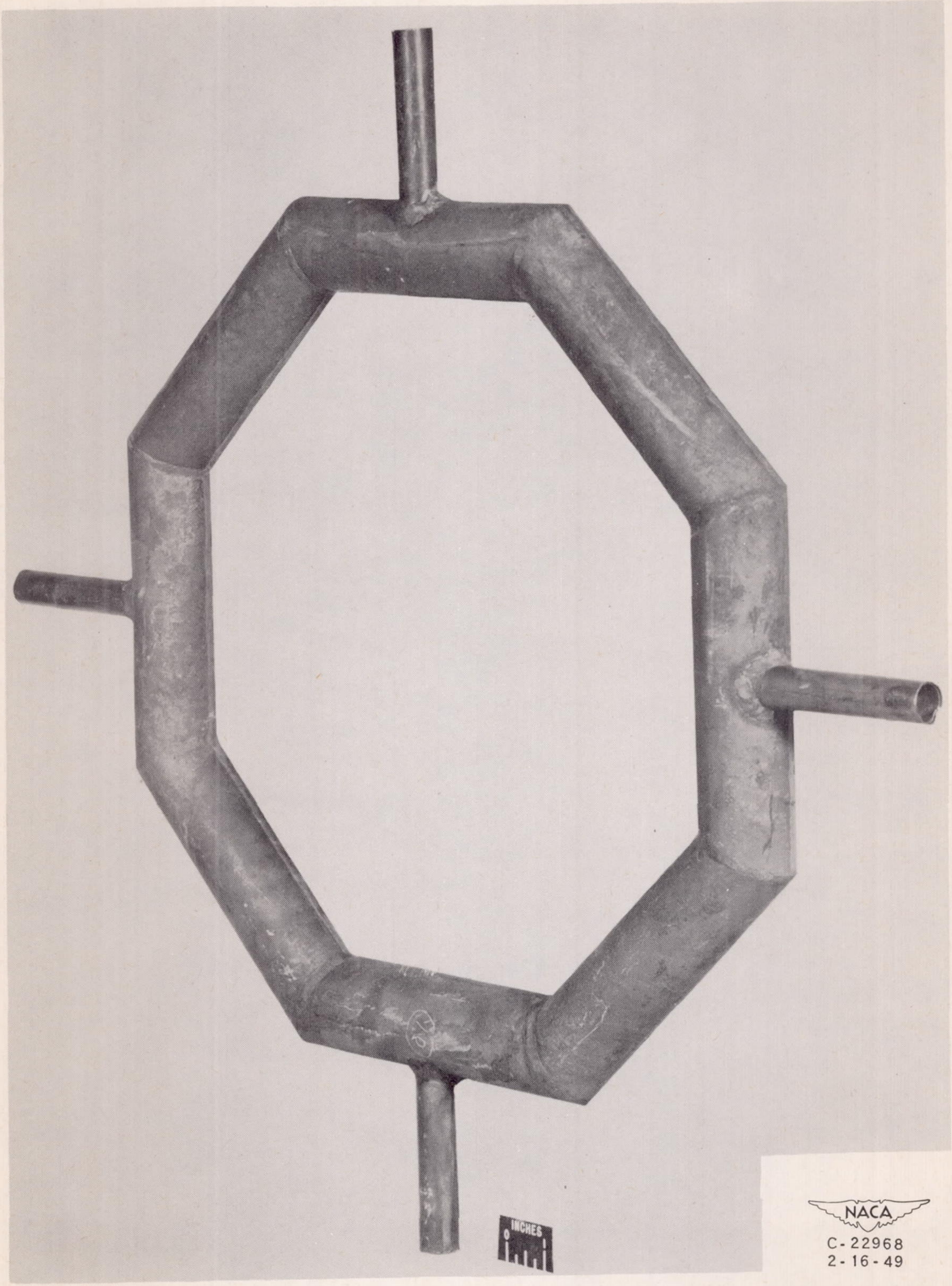
INCHES
0
1
NACA
C-22968
2-16-49

(b) Octagonal flame holder.
Figure 5. - Continued. Photographs of flame holders.

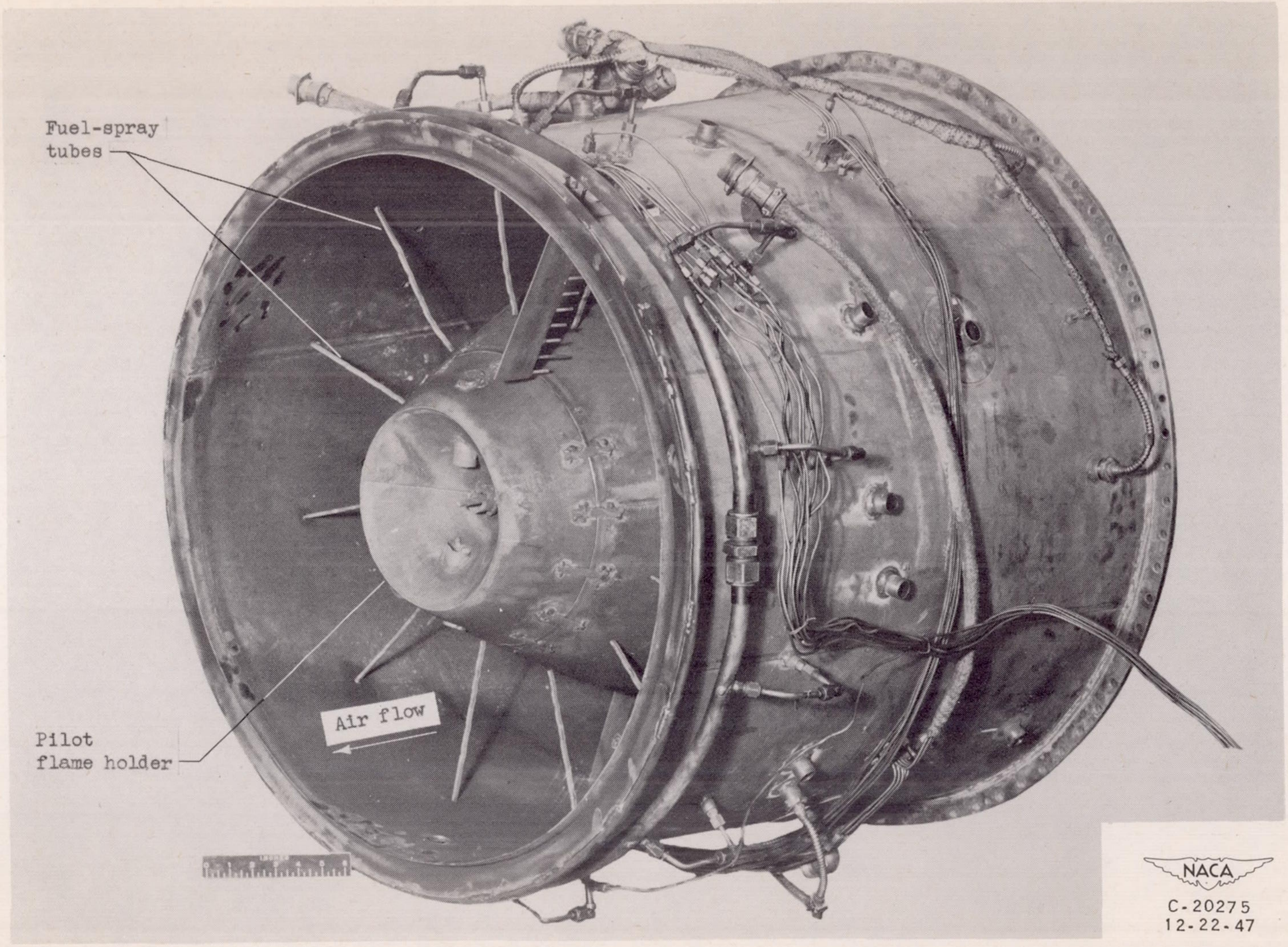
Fuel-spray tubes
Pilot flame holder
Air flow
NACA
C-20275
12-22-47

(c) Diffuser assembly showing pilot flame holder.
Figure 5. - Concluded. Photographs of flame holders.

206-1617

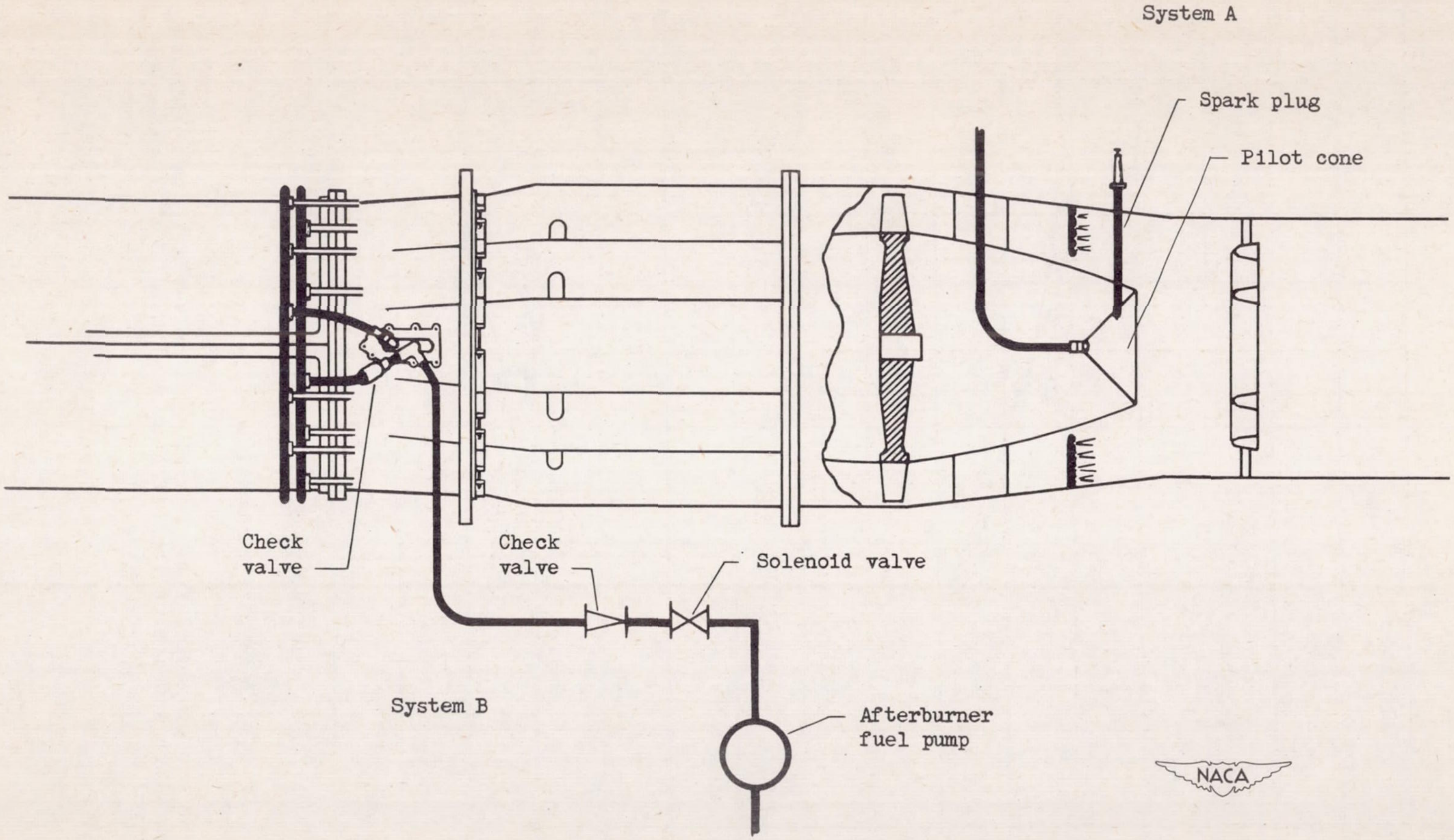
System A
Spark plug
Pilot cone
Check valve
Check valve
Solenoid valve
System B
Afterburner fuel pump
NACA

Figure 6. - Tail-pipe fuel-ignition systems.

1158

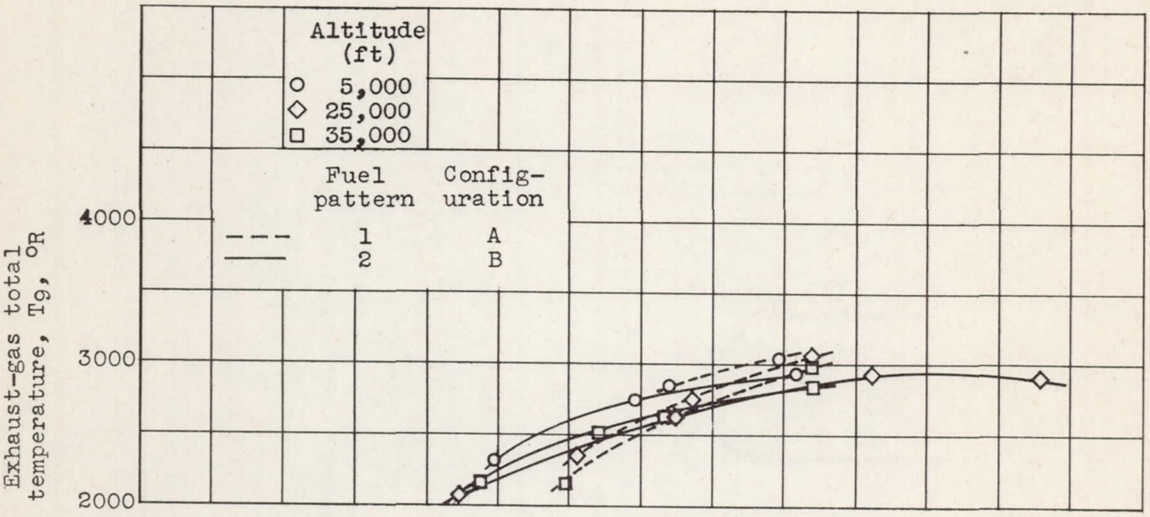

(a) Exhaust-gas total temperature.

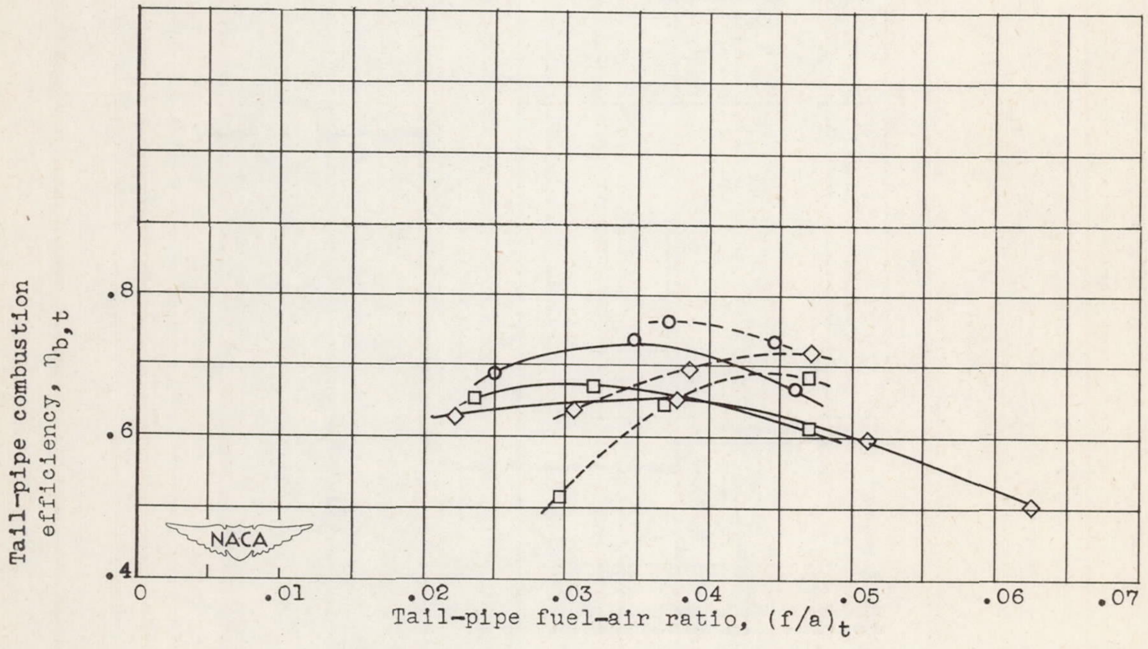

(b) Tail-pipe combustion efficiency.

Figure 7. - Effect of radial fuel distribution on variation of exhaust-gas total temperature and combustion efficiency with tail-pipe fuel-air ratio. Flight Mach number, 0.27.

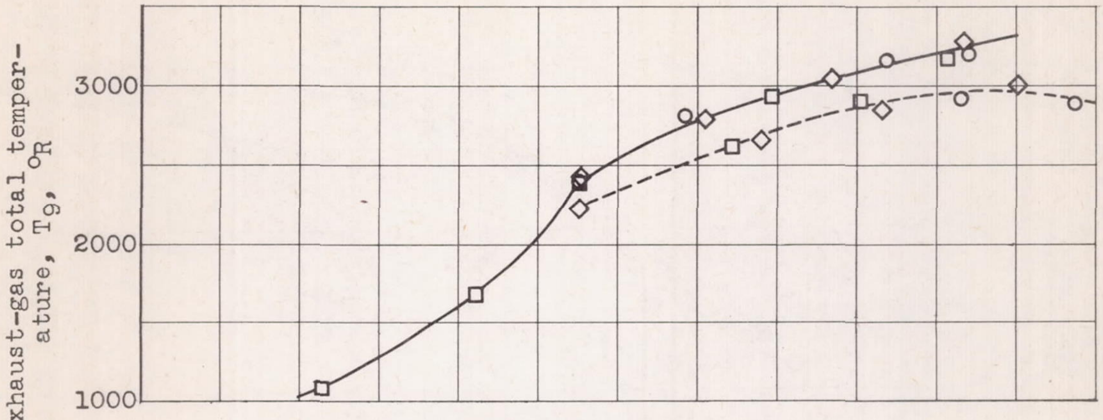

(a) Exhaust-gas total temperature.

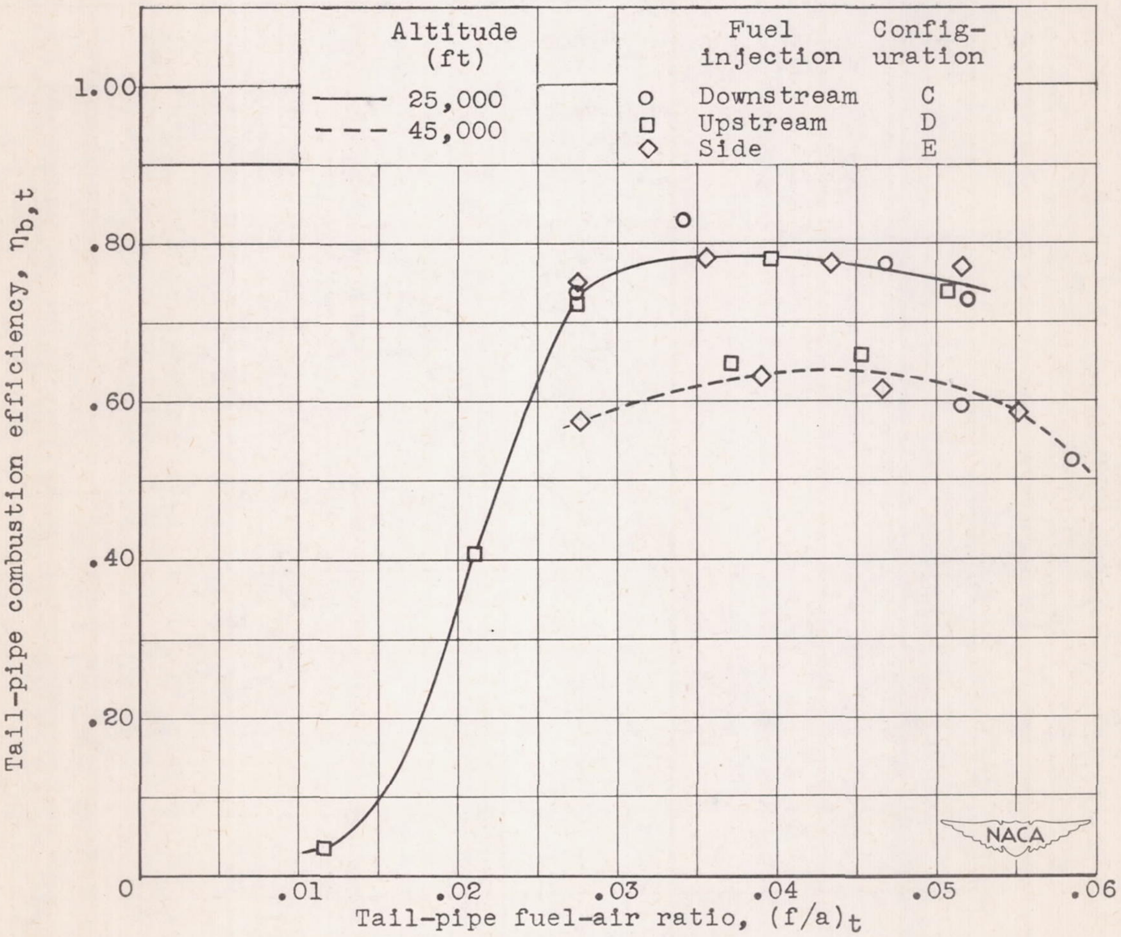

(b) Tail-pipe combustion efficiency.

Figure 8. - Effect of direction of fuel injection on variation of exhaust-gas total temperature and combustion efficiency with tail-pipe fuel-air ratio. Flight Mach number, 0.27; fuel pattern 3.

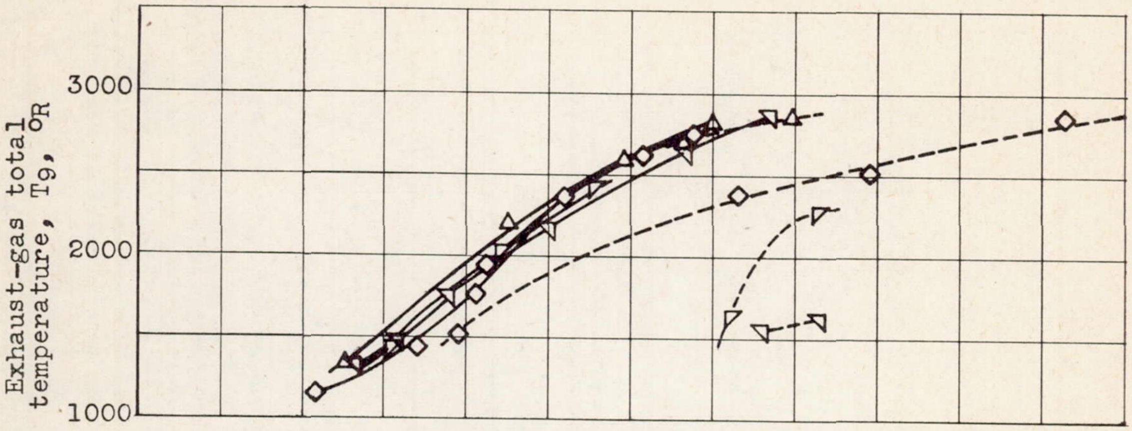

(a) Exhaust-gas total temperature.

1158

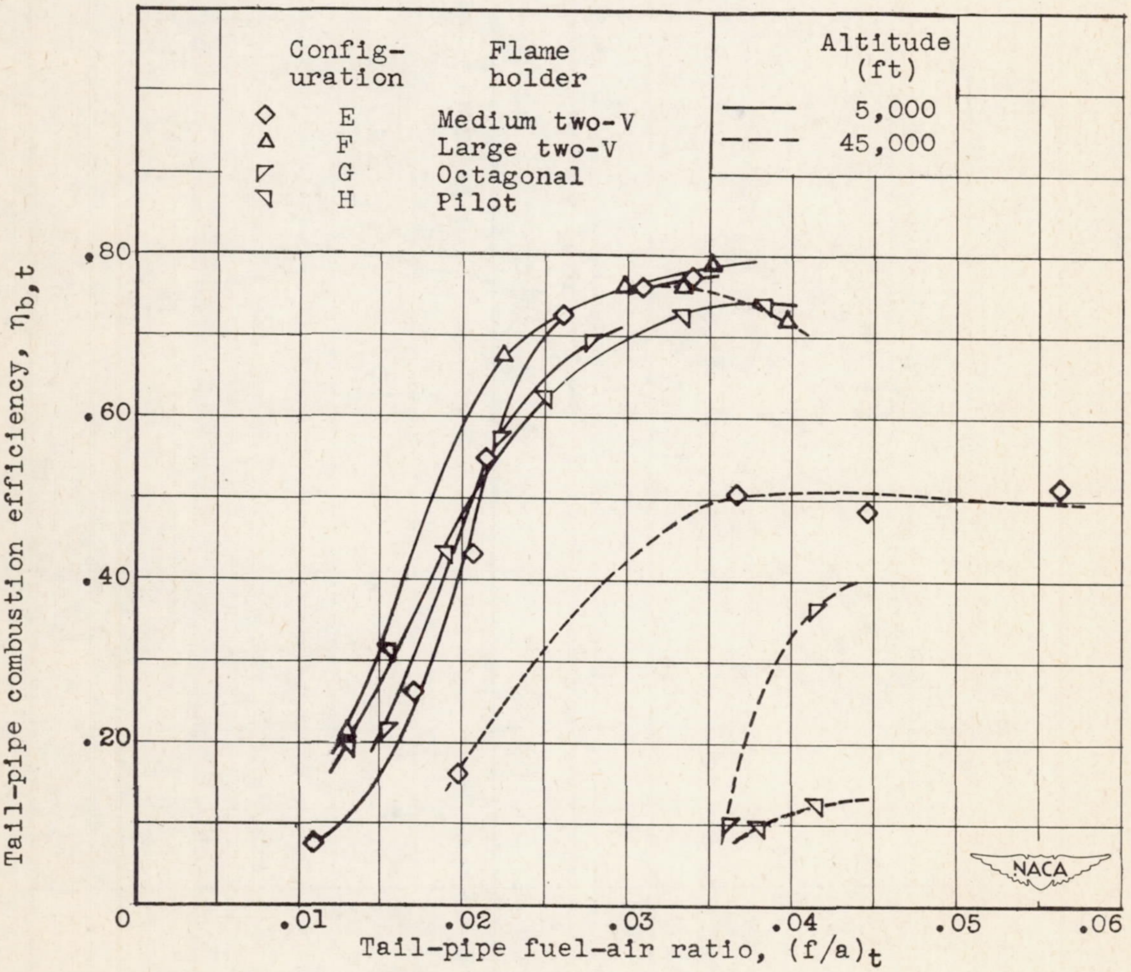

(b) Tail-pipe combustion efficiency.

Figure 9. - Effect of flame-holder design on variation of exhaust-gas total temperature and combustion efficiency with tail-pipe fuel-air ratio. Flight Mach number, 0.27.

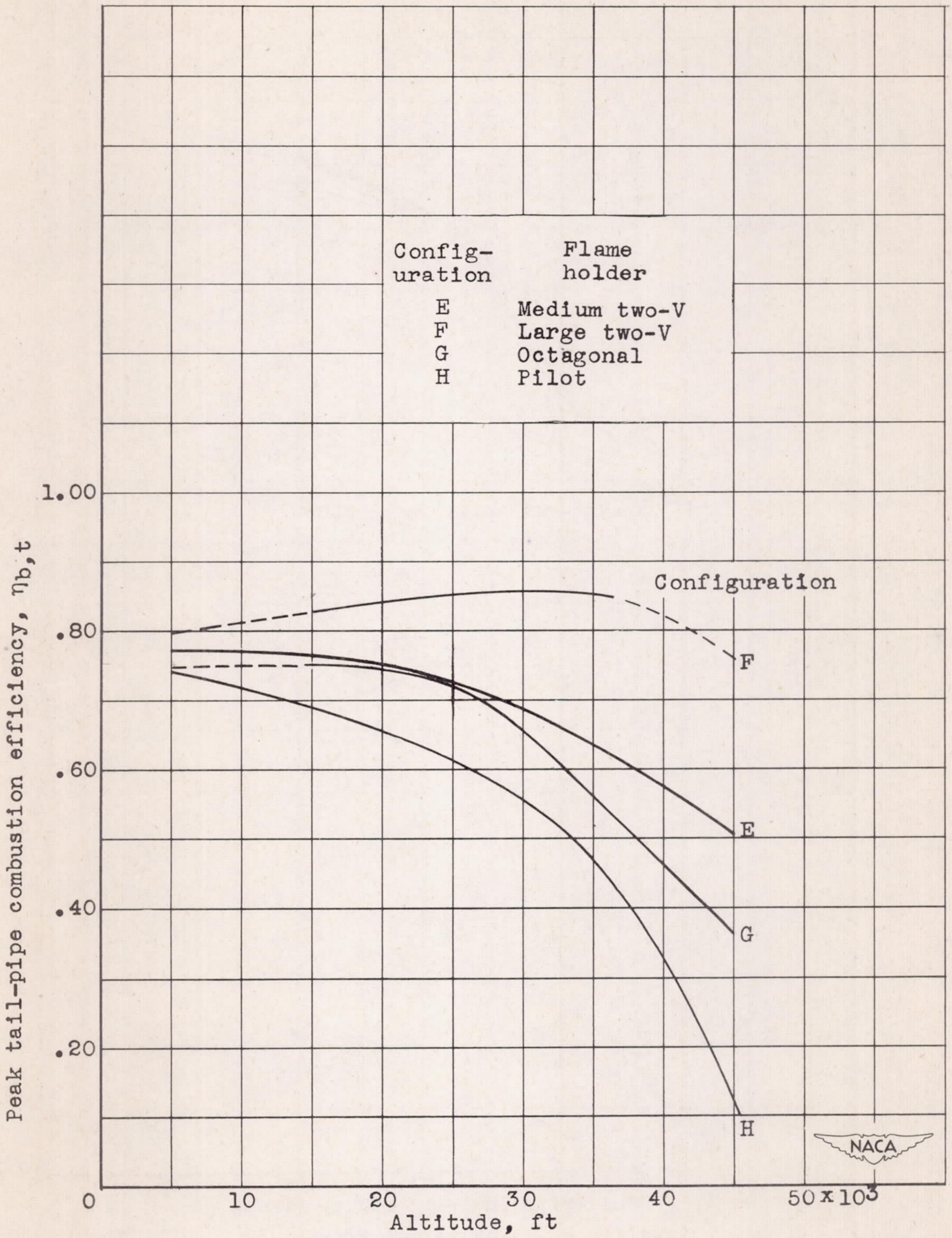

Figure 10. - Effect of flame-holder design on variation of peak combustion efficiency with altitude. Flight Mach number, 0.27.

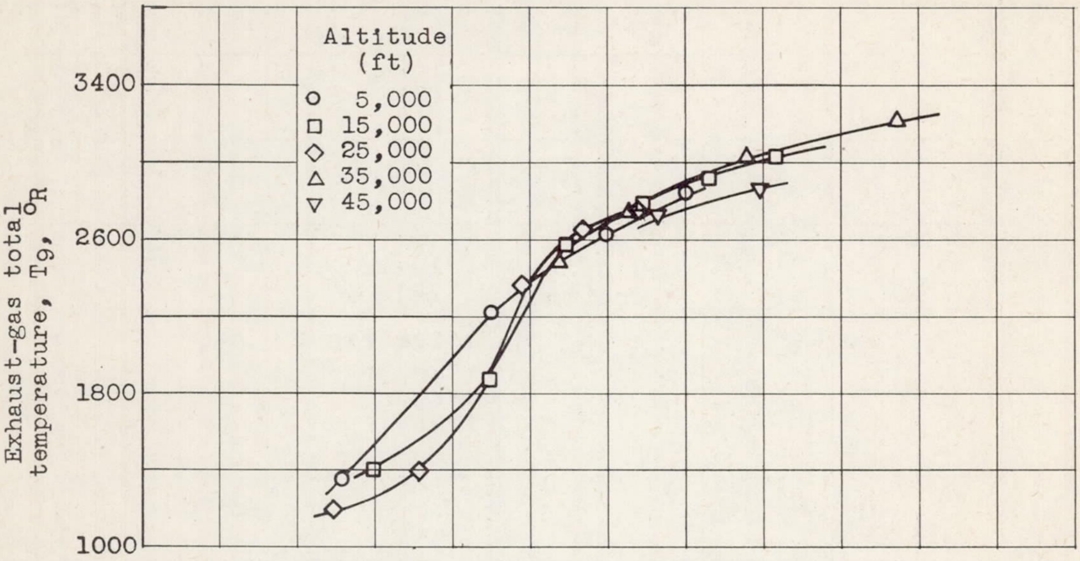

(a) Exhaust-gas total temperature.

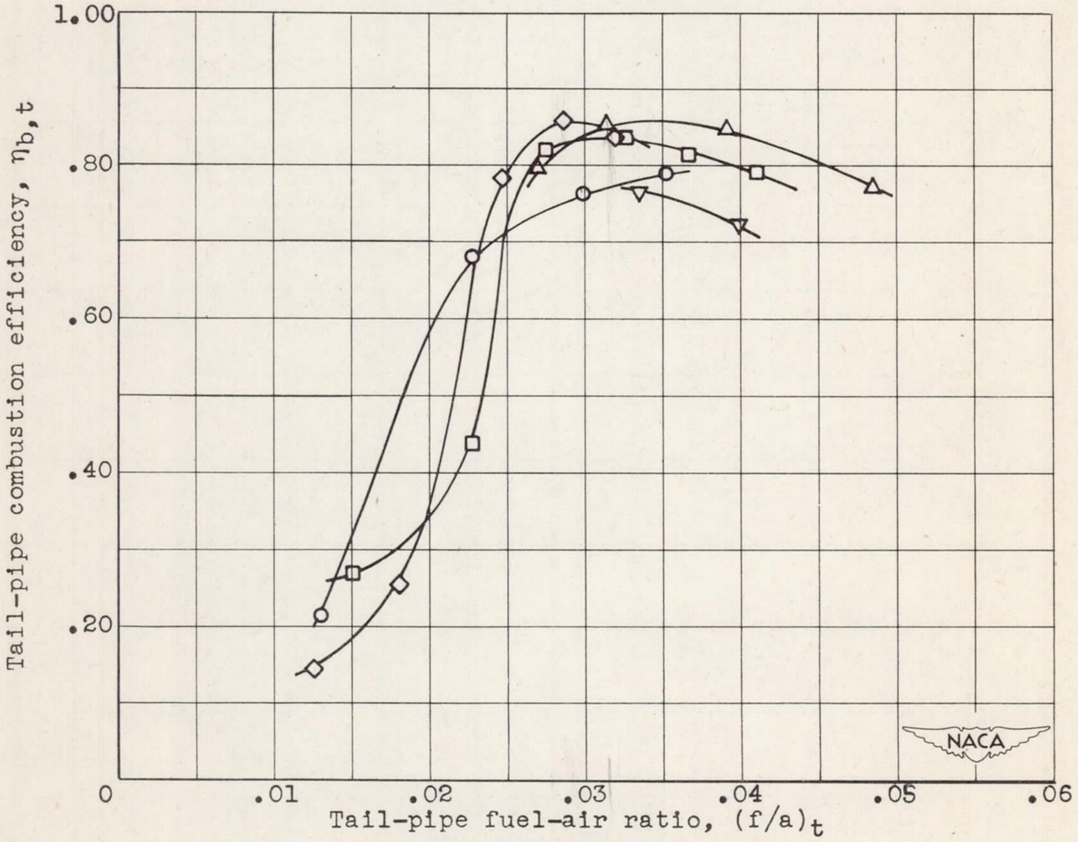

(b) Tail-pipe combustion efficiency.

Figure 11. - Effect of altitude on variation of exhaust-gas total temperature, tail-pipe combustion efficiency, and burner- and combustion-chamber-inlet conditions with tail-pipe fuel-air ratio for configuration F. Flight Mach number, 0.27.

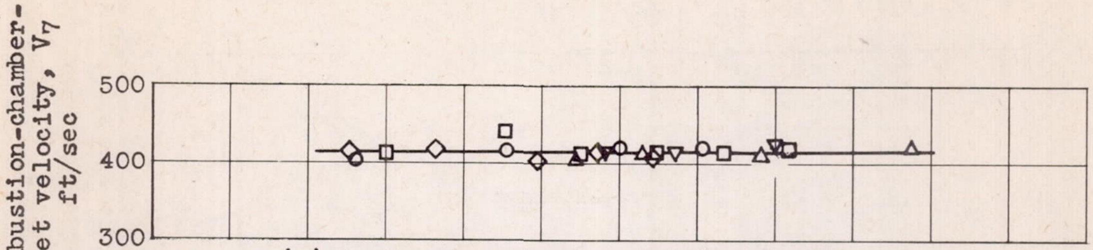

(c) Combustion-chamber-inlet velocity.

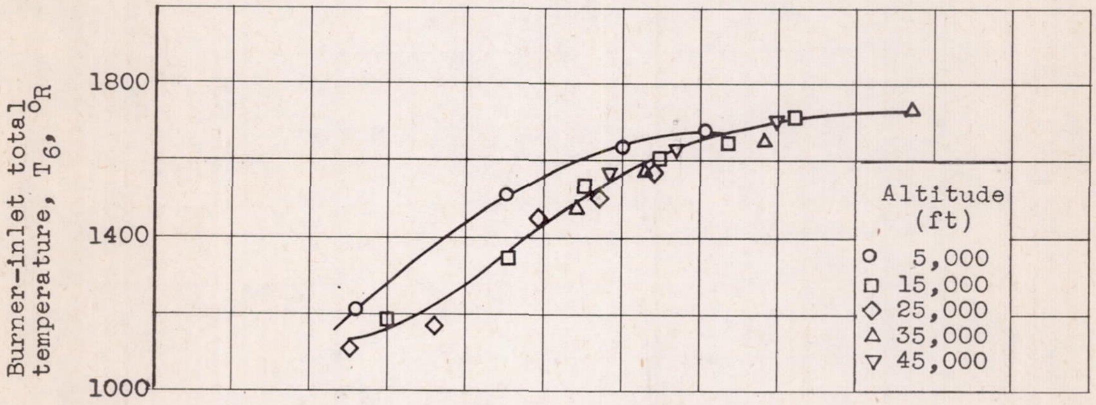

(d) Burner-inlet total temperature.

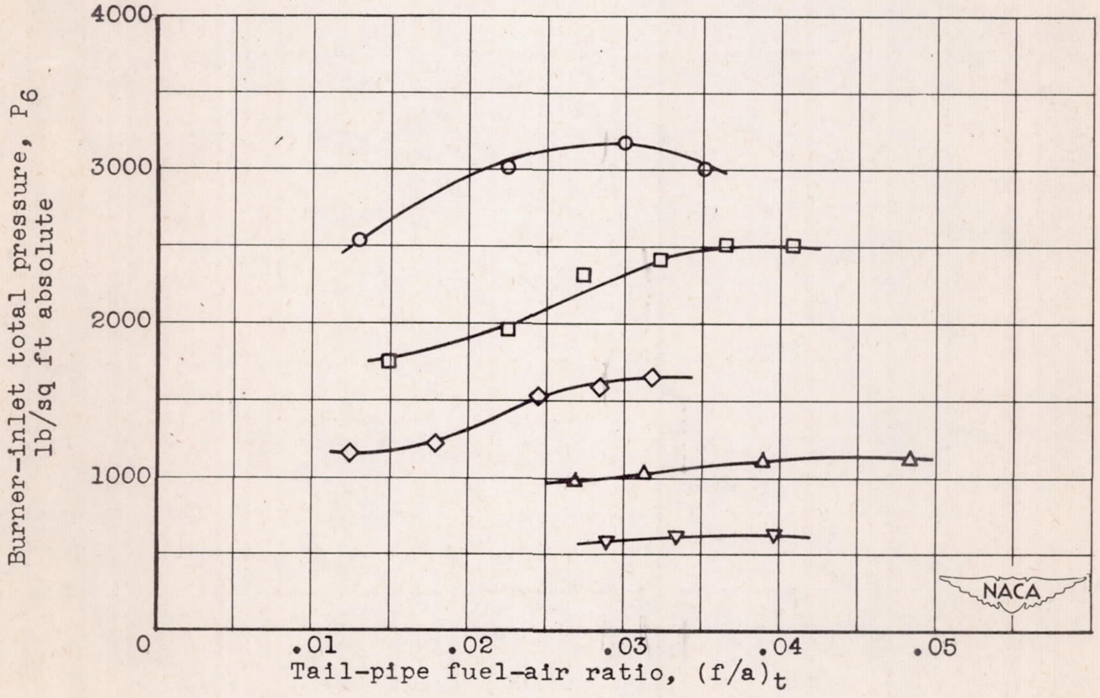

(e) Burner-inlet total pressure.

Figure 11. - Concluded. Effect of altitude on variation of exhaust-gas total temperature, tail-pipe combustion efficiency, and burner- and combustion-chamber-inlet conditions with tail-pipe fuel-air ratio for configuration F. Flight Mach number, 0.27.

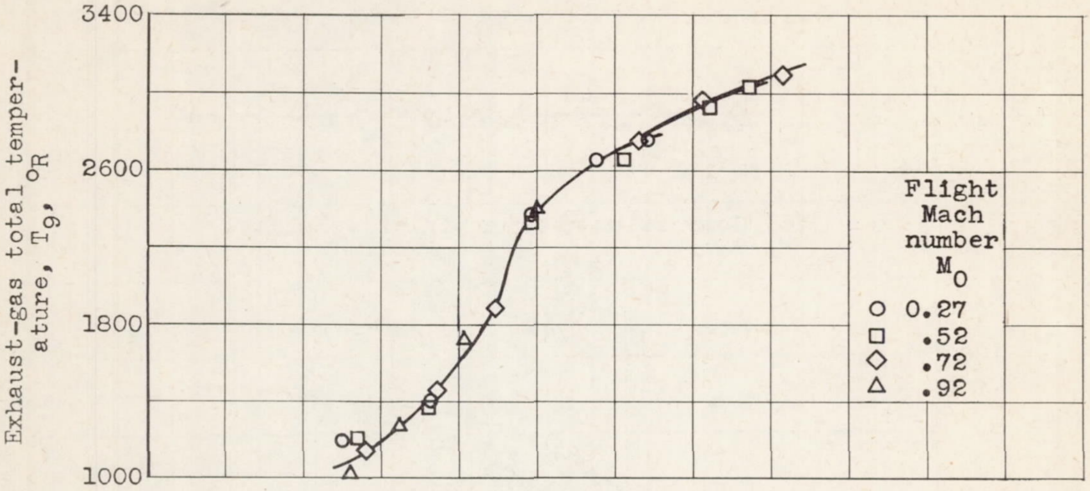

(a) Exhaust-gas total temperature.

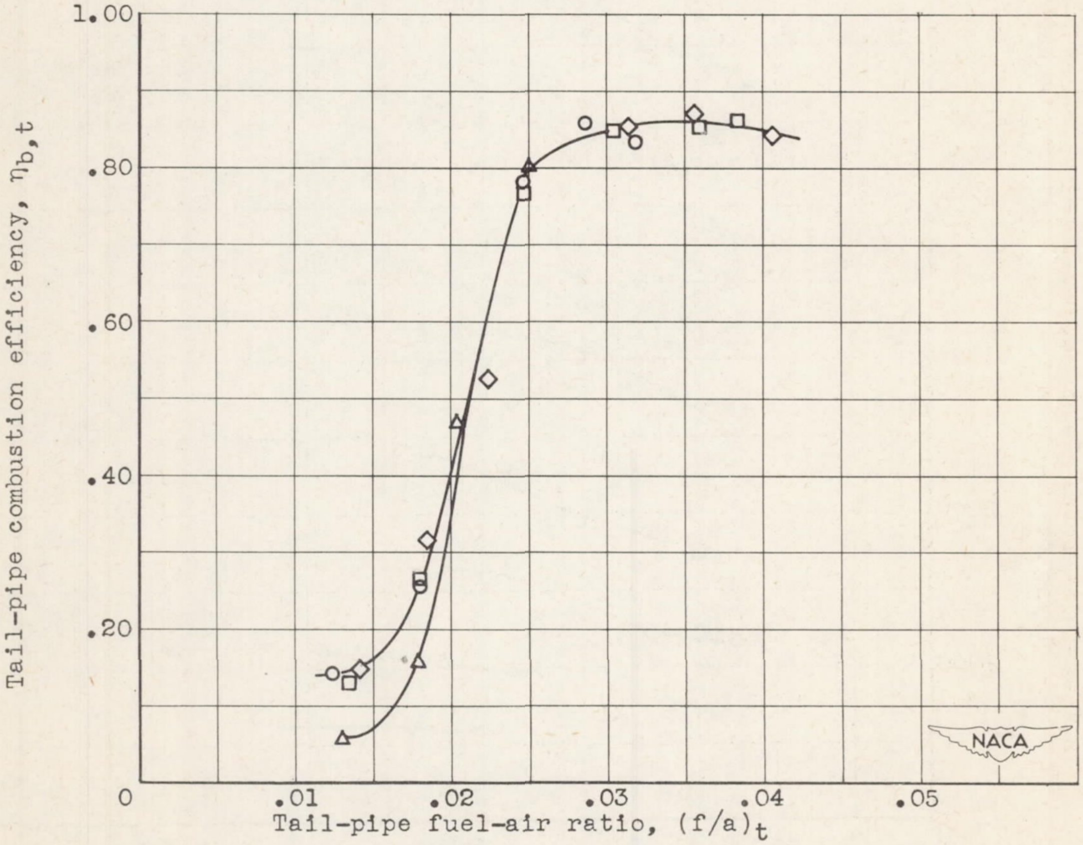

(b) Tail-pipe combustion efficiency.

Figure 12. - Effect of flight Mach number on variation of exhaust-gas total temperature, tail-pipe combustion efficiency, and burner- and combustion-chamber-inlet conditions with tail-pipe fuel-air ratio for configuration F. Altitude, 25,000 feet.

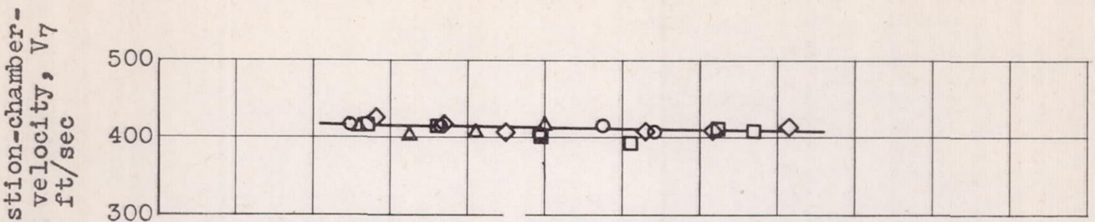

(c) Combustion-chamber-inlet velocity.

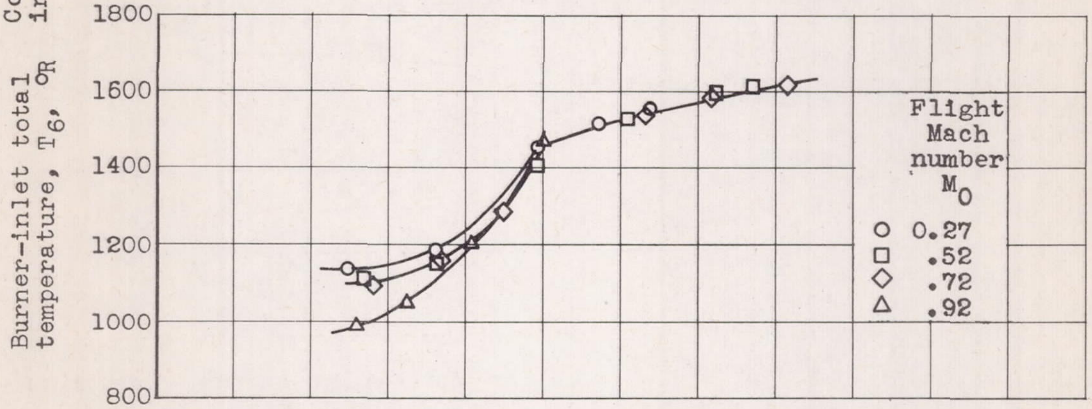

(d) Burner-inlet total temperature.

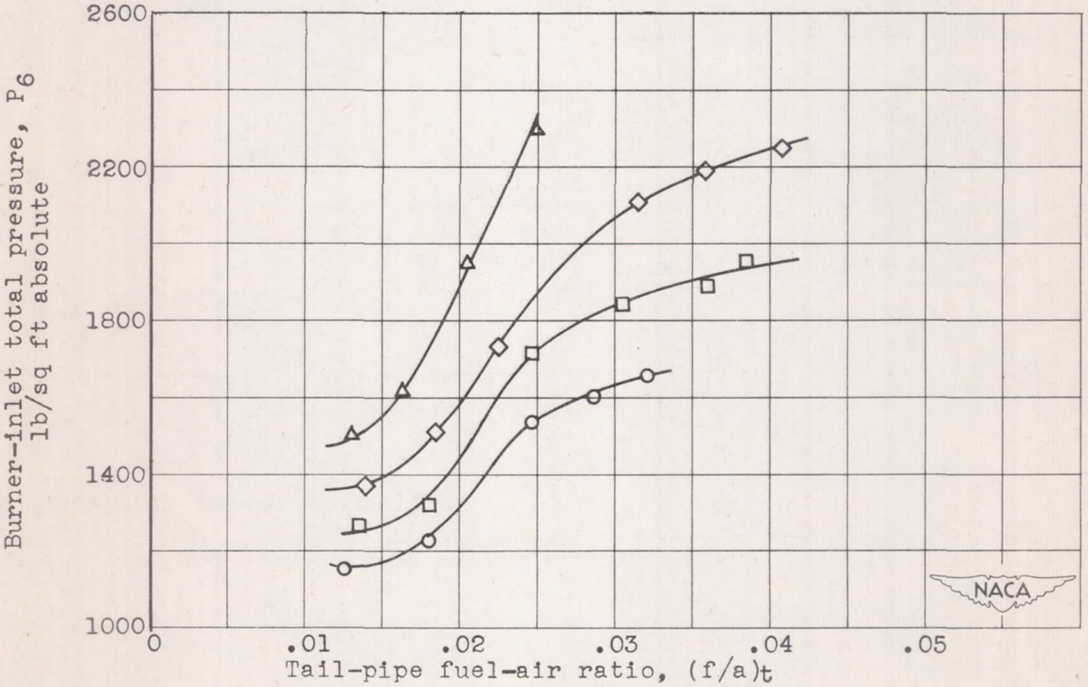

(e) Burner-inlet total pressure.

Figure 12. - Concluded. Effect of flight Mach number on variation of exhaust-gas total temperature, tail-pipe combustion efficiency, and burner- and combustion-chamber-inlet conditions with tail-pipe fuel-air ratio for configuration F. Altitude, 25,000 feet.

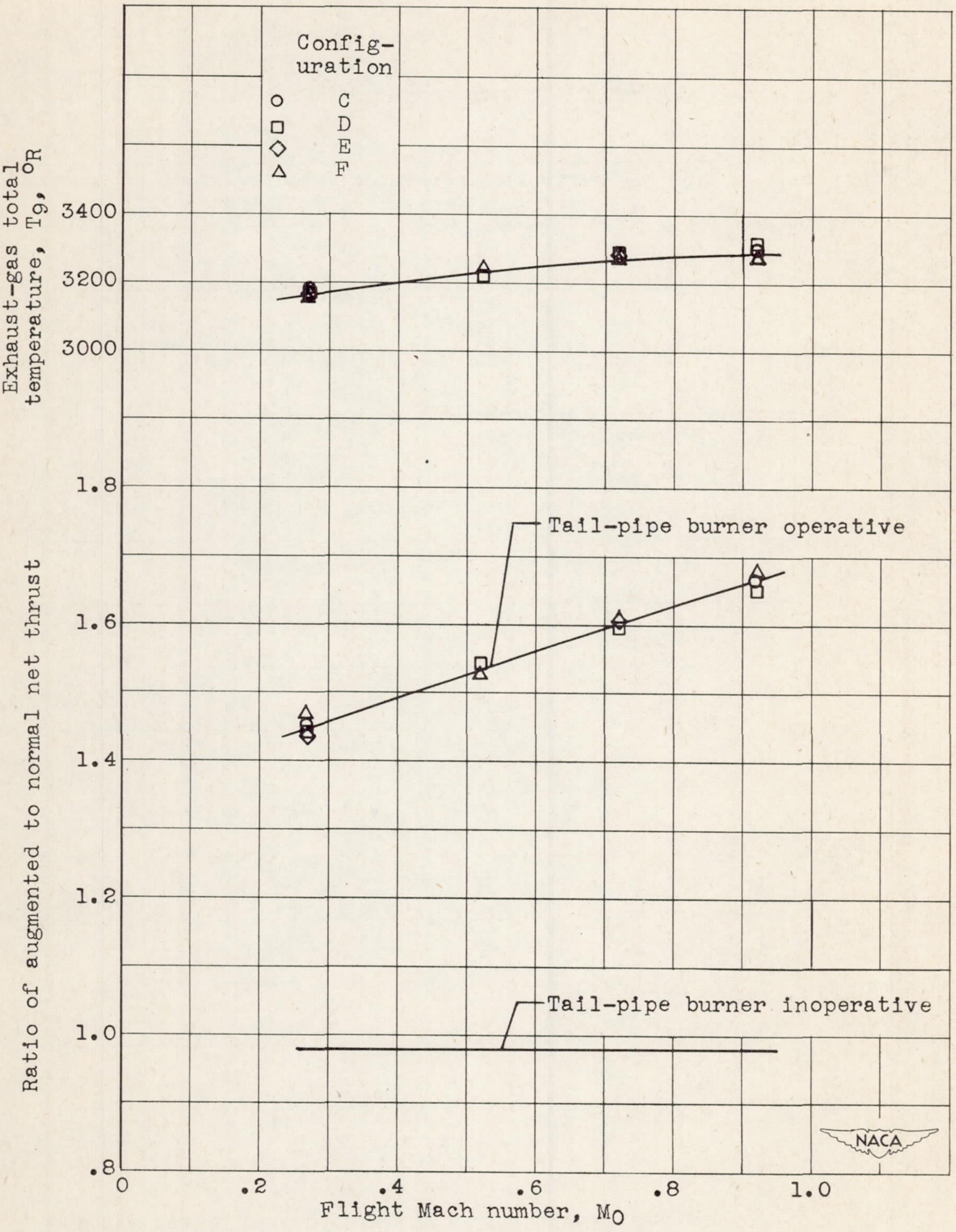

Figure 13. - Variation of thrust-augmentation ratio and exhaust-gas total temperature with flight Mach number for configurations C, D, E, and F. Turbine-outlet temperature, 1650° R; altitude, 25,000 feet.

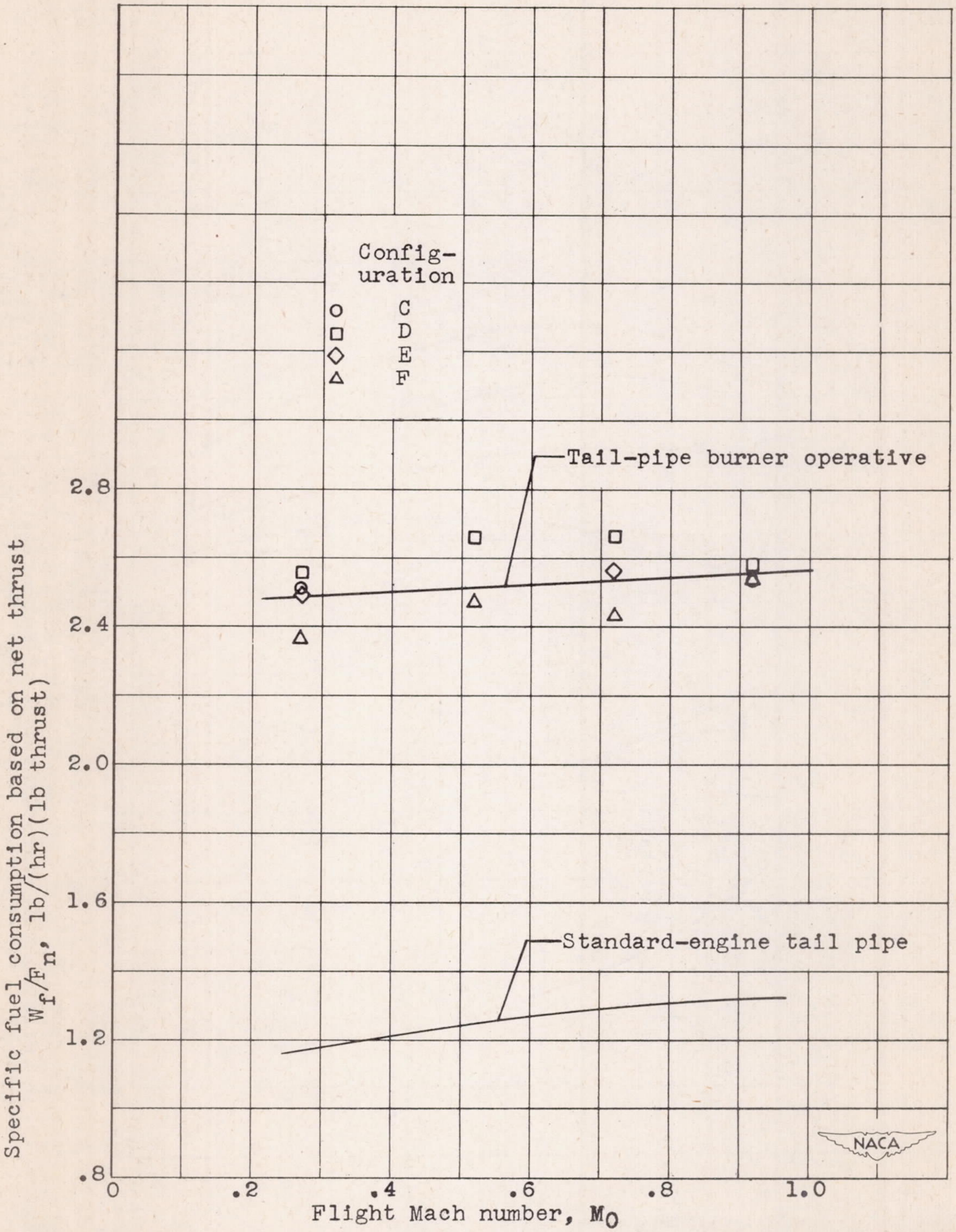

Figure 14. - Variation of specific fuel consumption based on net thrust with flight Mach number for configurations C, D, E, and F and for standard-engine tail pipe. Turbine-outlet temperature, 1650° R; altitude, 25,000 feet.

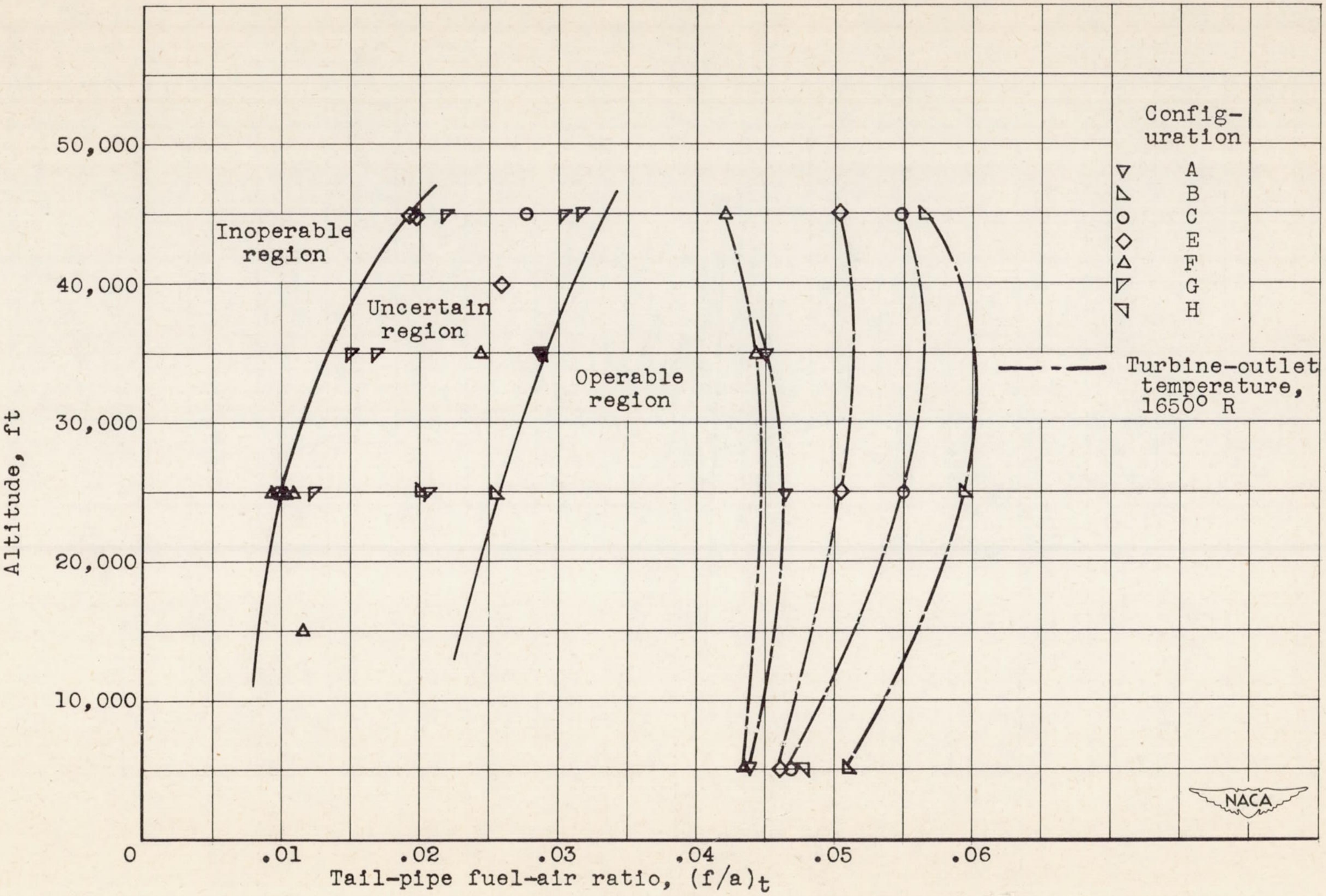

Figure 15. - Variation of operable range of tail-pipe fuel-air ratios with altitude for several tail-pipe-burner configurations. Flight Mach number, 0.27.